Analysis of a hybrid energy system for a new neighbourhood

Federica Marongiu

School of Engineering

Thesis submitted for examination for the degree of Master of Science in Technology.
Espoo 20.05.2020

Supervisor

Prof. Markku J. Virtanen

Advisor

MSc Riikka Pitkälä

Aalto University
School of Engineering

Aalto University
School of Engineering

Aalto University, P.O. BOX 11000, 00076 AALTO
www.aalto.fi
Abstract of the master's thesis

Author Federica Marongiu

Title Analysis of a hybrid energy system for a new neighbourhood

Master programme Building Technology **Code** ENG27

Supervisor Prof. Markku J. Virtanen

Advisor MSc Riikka Pitkälä

Date 20.05.2020 **Number of pages** 75 **Language** English

Abstract

Building sector accounts globally for the 36% of energy consumption and is responsible for the 39% of CO_2 emissions. Energy efficiency policies aim to lower the buildings' energy demand, but the change towards more sustainable solutions must include also the energy sector. Finland is already taking action towards lowering the use of fossil fuels in the energy production.

The main objective of this thesis is to analyse the feasibility of a local hybrid energy system. Geothermal energy is chosen as the main source for heating and cooling, while the additional energy is provided through district heating. As part of the system, a local low temperature network is used to supply the buildings. Research method is based mainly on simulations, through which energy demands, borehole field size and the local network performance are defined. Life cycle cost analysis and CO_2 emissions estimation are also carried out.

The best configuration for the borehole field resulted in a total of 154 wells, with a depth of 291 m. The proposed layout for the local plant would include three geothermal heat pumps, buffer tanks, district heating heat exchanger and free cooling equipment. With a heating output of 45°C, heat pumps are able to cover up the 70% of the total heat demand. According to the study, the local network seems to be able to deliver enough heating energy to the buildings, with supply temperatures ranging from 65 to 61°C.

The investment cost for a geothermal system is significantly high, and borehole drilling cost covers the 72%. However, for a life cycle of 25 years, the Net Present Value is positive and a payback period of 9.7 years would suggest that the investment is profitable. Compared to a case where all heating is provided via district heating, the annual purchased energy costs can be lowered up to 68% and CO_2 emissions would be reduced by 62%.

It appears that such system can fulfil the needs of the new neighbourhood and to reduce the emissions. However, site-specific data need to be used in the borehole field sizing and more detailed analysis on the investment costs must be conducted in view of future development.

Keywords Borehole thermal energy storage, Geothermal heat pump , Local network

Preface

This thesis was carried out in Bonava, which I want to thank for the opportunity. I want to thank all the people who have been advisors to me, Riikka Pitkälä, Jari Niemi and Tuula Honkala, for providing me with their knowledge and precious help in guiding me through this thesis.

Additionally, I would like to thank all the people who made this master's thesis possible. I want to express my gratitude to my supervisor, Professor Markku J. Virtanen, for advising and encouraging me, being always positive during all the thesis process. A special thanks goes to Mika Vuolle, for his significant help, and patience, in these months.

I want to thank my fellow students and friends, Viktoria, Laura and Jenni, for always being there and sharing all good and bad moments. A special thanks goes to Federica, for all the support she gave me especially in this complicated last period.

Finally, I want to thank my family, mum, dad and sister. Even if they are far away, their love and support made me reach this final step.

Espoo, 20.05.2020

Federica Marongiu

Contents

Symbols

$\Delta P/L$	$[kPa/m]$	Pipe pressure loss
ϵ	$[kgCO_2/MWh]$	Emission factor
λ_f	$[W/mK]$	Fluid thermal conductivity
λ_g	$[W/mK]$	Thermal conductivity of grout
λ_p	$[W/mK]$	Thermal conductivity of pipe
λ_s	$[W/mK]$	Thermal conductivity of ground
μ	$[kg/m\ s]$	Viscosity
ρ	$[kg/m^3]$	Density
$2S$	$[m]$	Shank spacing
B	$[m]$	Borehole spacing
C_{out}	$[kW]$	Heat pump cooling output
C_e	[€]	Energy costs
C_k	[€]	Annual costs
c_p	$[J/kg\ K]$	Specific heat
d	[%]	Discount factor
d_u/d_s	$[mm/mm]$	External/internal pipe diameters
E	$[kW]$	Heat pump electricity
e	[%]	Escalation
f	[−]	Friction factor
f	[%]	Inflation
H	$[m]$	Borehole depth
h	$[W/m^2K]$	Heat transfer coefficient
H_{out}	$[kW]$	Heat pump heating output
HL	$[W/m]$	Pipe heat loss
i	[%]	Nominal interest rate
I_k, I_0	[€]	Investment cost
L	$[m]$	Pipe length
M	[€]	Total maintenance cost
M	$[kg/s]$	Building mass flow
M_n	[€]	Yearly maintenance cost
n_d	[years]	Discounted payback period
Nu	[−]	Nusselt number
P_k	[€]	Annual profits
Pr	[−]	Prandtl number
q	$[W/m]$	Heat tranfer per unit length
Q_{DH}	$[MWh]$	District heating purchased energy
Q_{DHW}	$[MWh/a]$	Domestic hot water energy demand
Q_{HP}	$[MWh]$	Heat pump energy output
q_{min}	$[l/kW]$	Minimum water volume for buffer tank
Q_{peak}	$[kW]$	Peak load
Q_{SH}	$[MWh/a]$	Space heating energy demand
Q_i	$[MWh]$	Yarly energy consumption
q_m	$[kg/s]$	Watter mass flow rate

R	$[€]$	Residual value
r	$[\%]$	Real interest rate
$R*_b$	$[mK/W]$	Effective borehole thermal resistance
r_{eq}	$[m]$	Equivalent radius
R_{fc}	$[mK/W]$	Convective component of the pipe thermal resistance
r_{pi}	$[m]$	Pipe inner radius
r_{po}	$[m]$	Pipe outer radius
r_b	$[m]$	Borehole radius
R_b	$[mK/W]$	Fluid to ground thermal resistance
R_g	$[mK/W]$	Grout thermal resistance
R_p	$[mK/W]$	Pipe thermal resistance
R'_p	$[mK/W]$	Conductive component of the pipe thermal resistance
R_s	$[mK/W]$	Ground thermal reistance
R_t	$[mK/W]$	Total thermal resistance
Re	$[-]$	Reynolds number
S	$[m]$	Borehole center-to-pipe's center distance
$T_{b,ret}$	$[°C]$	Building return temperature
$T_{b,sup}$	$[°C]$	Building supply temperature
$T_{w,out}$	$[°C]$	Heat pump outlet water temperature
T_b	$[°C]$	Temperature at the borehole wall
T_f	$[°C]$	Borehole local mean fluid temperature
T_s	$[°C]$	Ground temperature
v	$[m/s]$	Fluid velocity
V_{BT}	$[l]$	Buffer tank volume

Abbreviations

AHU	Air Handling Unit
BH	Borehole
BHE	Borehole Heat Exchanger
BIM	Building Information Model
CHP	Combined Power and Heat
CO_2	Carbon Dioxide
COP	Coefficient Of Performance
DC	District Cooling
DH	District Heating
DHW	Domestic Hot Water
EED	Earth Energy Designer
EER	Energy Efficiency Ratio
EU	European Union
EWT	Entering Water Temperature
GHE	Ground Heat Exchanger
GSHP	Ground Source Heat Pump
GTK	Geologian Tutkimuskeskus
HP	Heat Pump
HVAC	Heating, Cooling and Air Conditioning
IEA	International Energy Agency
IFC	Industry Foundation Classes
LCC	Life Cycle Cost
LWT	Leaving Water Temperature
NPV	Net Present Value
SC	Space Cooling
SFP	Specific Fan Power
SH	Space Heating
SPF	Seasonal Performance Factor
TRT	Thermal Response Test
UBW	Uniform Borehole Wall (temperature)
UHF	Uniform Heat Flux
UTES	Underground Thermal Energy Storage

1 Introduction

1.1 Background

Globally, buildings and construction industry accounted for 36% of the final energy use and were responsible for 39% of energy- and process-related emissions in 2018 [1]. Standards on energy efficiency and energy labelling are nowadays in force, making the new constructions designed to be more energy efficient. An energy efficient building helps to reduce energy demand, therefore CO_2 emissions. But one has to consider that the current building stock (representing the 40% of EU energy consumption) will still exist in 2050: renovation is necessary, but needs important economic effort and proper planning. Together with buildings, energy systems and production need to face the transition towards greener and more sustainable solutions.

EU is actively working towards a reduction of emissions in every key economic sector. The target is now to reduce the emissions by 40%, compared to 1990 levels, by 2030 and becoming climate-neutral by 2050. One of the strategic points is "maximise the deployment of renewables and the use of electricity to fully decarbonise Europe's energy supply" [2]. By now, three EU countries have set their goal for carbon neutrality in law: Sweden, that aims to reach net-zero emissions by 2045, while France and the United Kingdom by 2050.
Finland has also set some ambitious goals. Helsinki city aims to become carbon neutral by 2035. A clean energy production, which will abandon coal progressively, is one of the points in the city program. Helen will reduce the district heating (DH) emissions of 74% by 2035. At the same time, the city of Espoo together with Fortum are committed to abandon the burning coal by 2025, which now represents the 50% of the total production. Replacing energy sources are going to be mainly waste heat and geothermal energy. One of the problems is, for example, the mismatch between the low temperature heat from industry and the current DH temperatures.

In Finland, DH represents 46% of the heating market [3]. In new buildings, DH represents the preferred mean for the heat supply. The 65% of new residential buildings are connected to the DH network, among which 95% of the apartment buildings and 11% of detached houses. The share of commercial buildings, buildings for institutional care and office buildings connected to DH are, respectively, 66%, 84% and 87%.
The trend in DH production shows the change towards more sustainable fuels: in 10 years (2009-2019), the renewable share has increased up to 42% and heat recovery (waste heat) to 10%. Figure 1 shows the 2019 share of energy sources in DH production.

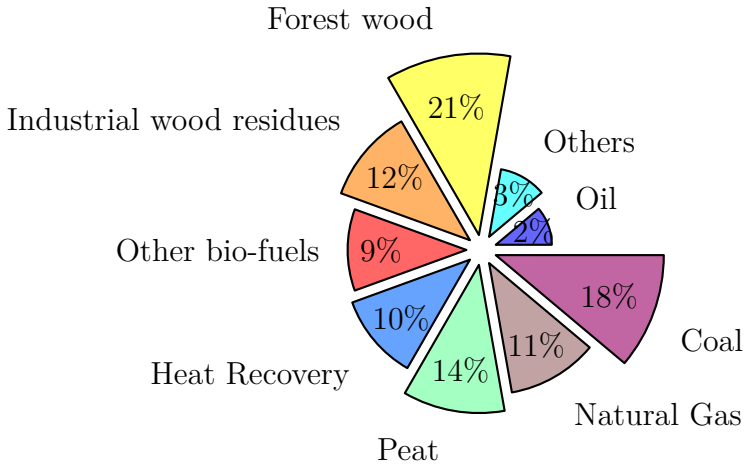

Figure 1: District heating production fuels

District cooling (DC) is, instead, produced mainly through heat pumps (66%) and free cooling (21%).

The need to integrate renewable sources, reduce energy waste and improve efficiency, sets the basis for the evolution of the district heating towards its fourth generation (4GDH) [4]. The new district heating has several advantages both in distribution and production. Low supply temperature reduce distribution losses and allows the use of smaller pipe diameters. Low grade energy sources, which temperatures until now were too low, can in this asset be integrated into the production. Waste heat from industrial processes and from cooling in commercial buildings have a high potential to be utilised, as well as geothermal heat and solar heating plants. Low supply and return temperatures increase also the efficiency at production level, resulting in higher power-to-heat ratios in Combined Heat and Power (CHP) plants, higher heat recovery from flue gas condensation and higher Coefficient of Performance (COP) in heat pumps.

The implementation of low temperature systems is limited by the existing energy infrastructure and the high temperature distribution systems in the buildings, thus is still far from being applied on a large scale. Anyhow, the problem is overcome when the system is installed in new building areas, more energy efficient and where floor heating is utilised. There have been pilot projects, where low temperature district heating have been implemented in small residential communities. Among the case studies reported by IEA [5], two projects developed in Germany are of particular interest.
A residential area in Wüstenrot utilises geothermal energy for both heating and cooling. Agro-thermal collectors are installed at a depth of 2 m. The low temperature heat collected is circulated through the network and the heat is provided to the buildings through decentralised heat pumps. The collectors can also function as free cooling source during summer.
The second example is the area "Zum Feldlager" in Kassel [6]. Amongst the different

variants analysed, one proposed solution is to have a centralised geothermal heat pump, which supplies the district heating network at 40°C, while unglazed solar collectors take care of soil regeneration. Domestic hot water can either be prepared with solar thermal collectors or a heating rod.

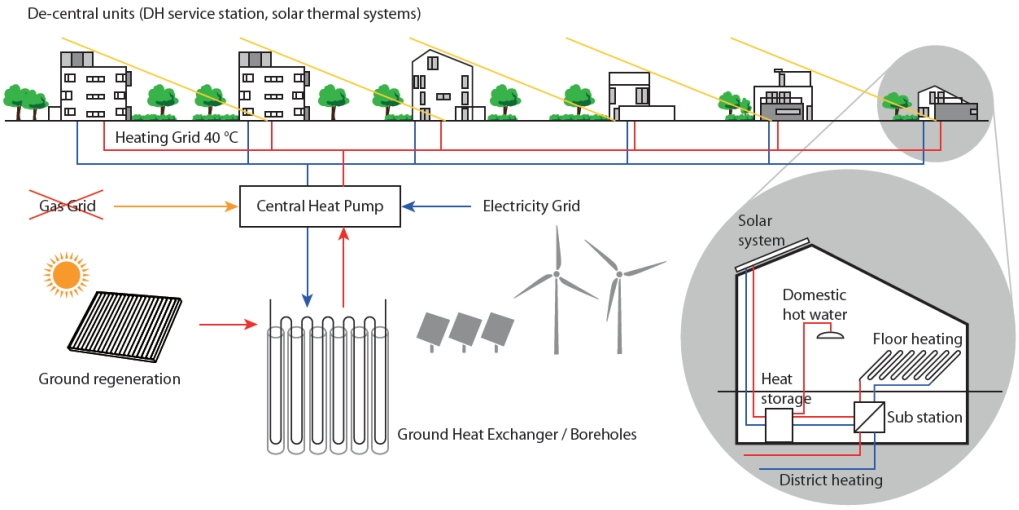

Figure 2: Scheme of geothermal solution for Kassel area [5]

1.2 Main objectives and scope of the thesis

The aim of this research is to analyse the feasibility of a local district heating and cooling network in a new neighbourhood, with a centralised supply plant which will be located directly in the area. This thesis work explores the possibility of utilising geothermal energy as the main source of heating and cooling, while supplying the buildings with a low temperature district heating network.
Therefore, the scope is to analyse an alternative to the conventional heat supply through district heating, by utilising energy produced on-site. However, a backup for peak loads will be needed. Typically, when operating geothermal heat pumps, the backup is provided through electric boilers. This research instead, aims to analyse the situation when the backup is represented by district heating. Within this framework, three are the main research questions:

1. What is a possible layout for a centralised heating and cooling plant for this area?

2. Is such hybrid system, together with a low temperature network, able to satisfy the heating demand of the area?

3. What are the costs of this system and are there savings when compared to a traditional district heating connection? How big is the impact in terms of CO_2 emissions?

The starting point is the calculation of buildings' energy demand. Dynamic simulation approach has been chosen to determine the demand of the apartment buildings,

while a standardised load profile from a previous research has been used for the office building.
Once the total site demand has been defined, decision has been made upon the percentage of peak load that the geothermal heat pumps are wanted to cover. Then, solutions for geothermal field are simulated, including only space heating supply, when the domestic hot water is included and with and without active cooling. The best solution has been chosen with the criteria of shorter length and available temperatures after 25 years.
A layout for the centralised plant is proposed, comprising the hybrid heating connection and the free cooling. At the same time, the distribution network for the area has been sized. It comprises a four-pipe system, two pipes for heating (space heating and domestic hot water) and two for cooling.
A network model is also developed in IDA ICE. A first model simulates a traditional district heating supply. Afterwards, a plant which includes the borehole field, based on the data coming from the Earth Energy Designer (EED) simulation, and the and the hybrid system has been modelled, in order to see their behaviour together with the network.
Once all the components of the system (boreholes, network, energy centre), the cost estimation has been carried out and a comparison between a district heating only system and the one with geothermal energy source integrated is made. Based on energy consumption, a rough estimation of the CO_2 emissions is also carried out.

1.3 Structure of the thesis

The thesis, besides the introduction and conclusion, is organised in five sections:

Chapter 2 explains how the energy demands are defined for the two building typologies, and for the total plot. The results are also presented.

Chapter 3 contains a literature review on the ground heat exchangers. It focuses on borehole heat exchangers, reviewing the different methods to define its resistance, the interaction with the ground and, briefly, design considerations on borehole fields.

Chapter 4 is dedicated to the case study and it is divided into three sections. In the first one, the borehole field for the area is defined and simulation results from EED are presented. The second section is about the heating and cooling plant, its components and layout. The third section concerns the local energy network, and its simulation model developed in IDA ICE.

Chapter 5 deals with the economic aspect and costs, comparing the operational costs when using only district heating and when implementing the heat pumps (HPs). Moreover, a rough estimation of the CO_2 emissions is carried out.

Chapter 6 summarises and discusses the main results of the simulations and the Life Cycle Cost (LCC) calculations.

2 Heating and cooling demand definition

This chapter describes the definition of the heating and cooling demands of the two building typologies present on the plot, residential and office building, and the total site demand.

The building type determined the level of detail of the information available, which affected the choice on the method through which the energy demand was defined. For the residential buildings, a dynamic simulation model was used; the office building consumption is based on standardised load profiles; the total site demand is obtained through the superposition of these two load profiles.

2.1 Apartment building demand

The residential buildings in this project cover an area of approximately 90 000 m^2. The starting point for the definition of their heating and cooling energy demand, is a model building (MB) for which a building information model (BIM) is available. Due to the preliminary phase in which the project is at the moment, the MB is enough to define the specific heating and cooling demand, since it is representative of the standard production of the housing company.

The MB is an 8 storey building, with a net heated area of about 4600 m^2. The first floor contains the common areas, the cellars and technical spaces. The apartments are located in the upper floors, all with the same 11 units layout, divided in stairs A and B, for a total of 77 apartments.

The main features of the heating, ventilation and air conditioning (HVAC) system comprise: ventilation system, which provides for an air handling unit (AHU) for each apartment, equipped with an electric heating coil and rotary heat recovery; the heating system is hydronic underfloor heating, except in the bathrooms, where the floor heating is electric; cooling is distributed through the same underfloor piping used for heating.

2.1.1 Model description

The choice for the simulation software fell on IDA ICE, a well validated dynamic simulation software. The BIM model makes the import into IDA ICE fairly easy, through the IFC format. Prior to the import, structural, window, door and room/zone types should be defined, so that they can be mapped to the ones in the model during the import.

The geometry of the model is based on the IFC model, meaning that the zones in IDA correspond to the ones defined in the BIM model.

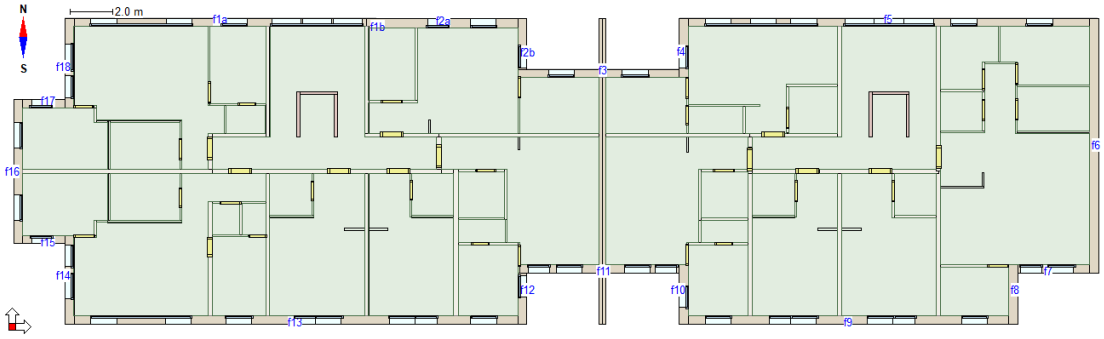

Figure 3: Apartment layout in IDA ICE

The structures are defined according to the architect's drawings. During the import, the option to merge the windows has been used. This allows to speed up the simulation time without affecting the results. U-values are summarised in Table 2. Weather data used is Helsinki-Vantaa TRY2012 reference year.

Table 2: Envelope U-values

External walls	0.16 W/m^2K
Roof	0.09 W/m^2K
Floor towards ground	0.16 W/m^2K
Windows & doors	1 W/m^2K

This Detailed Model (DM) contains 319 zones, one for each room in the building, but not all of them are actually inserted: only four floors were modelled (1st, 2nd, 5th and 8th), the remaining are copies of the 5th floor, by means of a room multiplier.

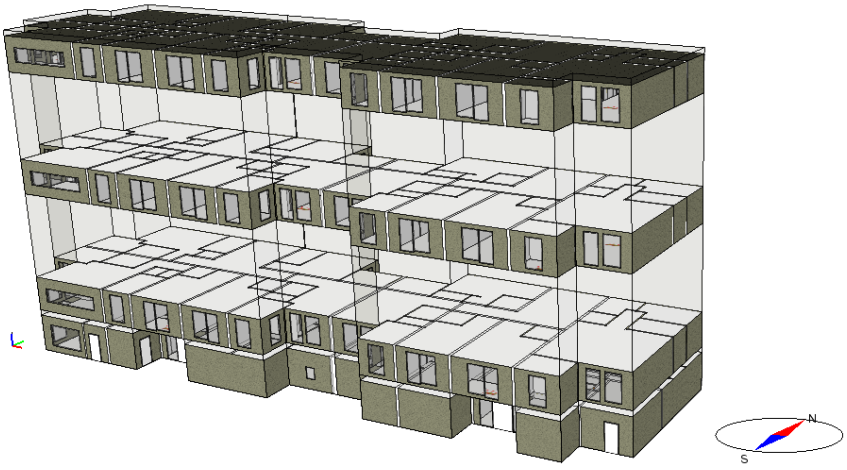

Figure 4: 3D model, with room multiplier in use

Once geometry has been defined, the HVAC system must be modelled and the internal gains defined.

The ventilation system comprises only one AHU, with electric heating coil. The Specific Fan Power (SFP) is calculated as $SFP = P/q_{extract}$, where P is the electric power input, in W, and $q_{extract}$ is the air flow rate, which corresponds to 0.5 dm^3/sm^2. The efficiency of the heat exchanger is calculated according to the Ministry of the Environment spreadsheet "LTO-laskin 2018, joulukuu 2017". The SFP results 1.36 $kW/(m^3/s)$, while the heat recovery efficiency is 79.9%.
Heat distribution is realised through hydronic underfloor heating and electric underfloor heating for the bathrooms. As cooling system, the same underfloor pipes are used.

In order to define the heating and cooling demand the standard plant is used, where the energy carrier is district heating and cooling. Space heating supply follows the heating curve in Fig. 5, while the set point for cooling is chosen as 18°C supply water temperature.

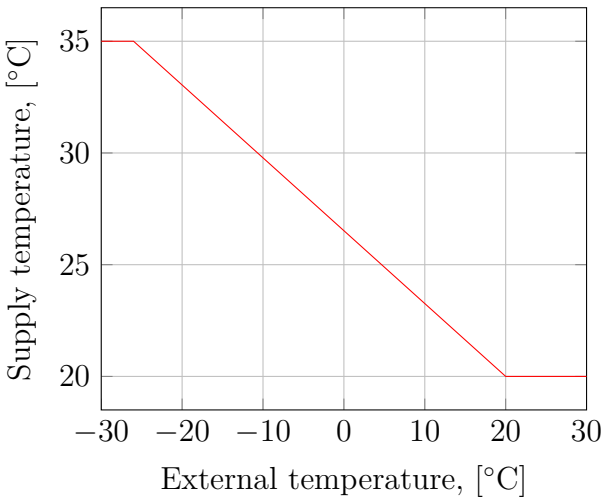

Figure 5: Supply temperature control for heating

The schedules for occupancy, lights and equipment are defined based on FINVAC guidance [7], in order to obtain a variation of the internal gains, so that the load profile does not only depend on external temperature and solar radiation variations. As an example, the regulation states that the occupancy gain is 3 W/m^2 and it is distributed over the 24 hours with a constant utilization rate of 60%. With the utilised profiles, the overall load stays the same but a bedroom will be occupied only during night hours, while the kitchen and living room only during meal hours, reflecting typical living habits. Same goes for lighting and consumer equipment, including weekday-weekend variations.

The same approach has been applied to domestic hot water. Its consumption is estimated by the regulation to be 35 kWh/m^2a, equivalent to $600l/m^2a$. The latter value is used in the simulation and the profiles modelled by Ahmed et al. [8] are applied. In this research, hourly profiles are estimated based on real consumption measurements, conducted on an apartment building located in Helsinki. Hourly

consumption factors are derived for winter and summer, and also differentiated between weekdays and weekends. Here, the factors for a group of more than 50 people are used. They define how the total water consumption is distributed throughout the day, hour by hour.

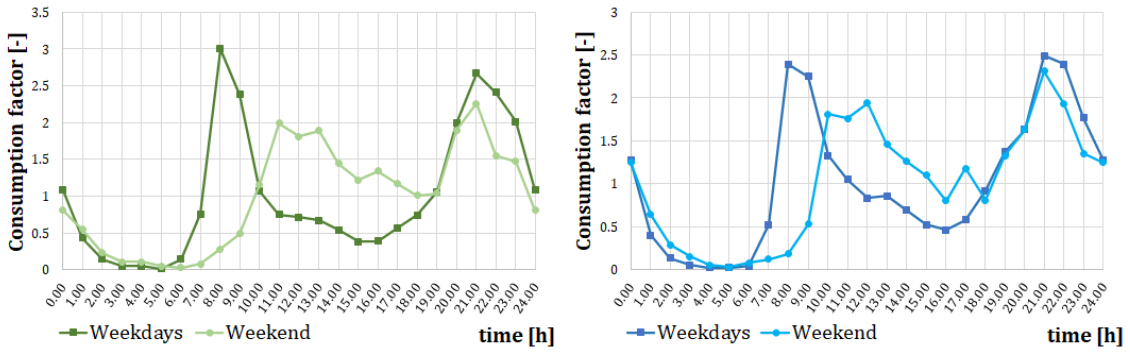

Figure 6: Consumption factors for winter (left) and summer (right)

2.1.2 Model building's energy consumption

Simulated energy consumption of the building results in 254143 kWh/a for heating, consisting in 68483.2 kWh/a for space heating and 185659.7 kWh/a, while cooling accounts for 20214 kWh/a. Corresponding load profiles are shown in Figure 7. Only water-based energy demand is considered in this study, therefore the demand for electrical floor heating and ventilation heating is not reported.

The building presents an E-figure is 84 kWh_E/m^2a, classifying the building in class B, according to current regulation. This result is in line with other projects from the same company, which range is between 80 and 86 kWh_E/m^2a.

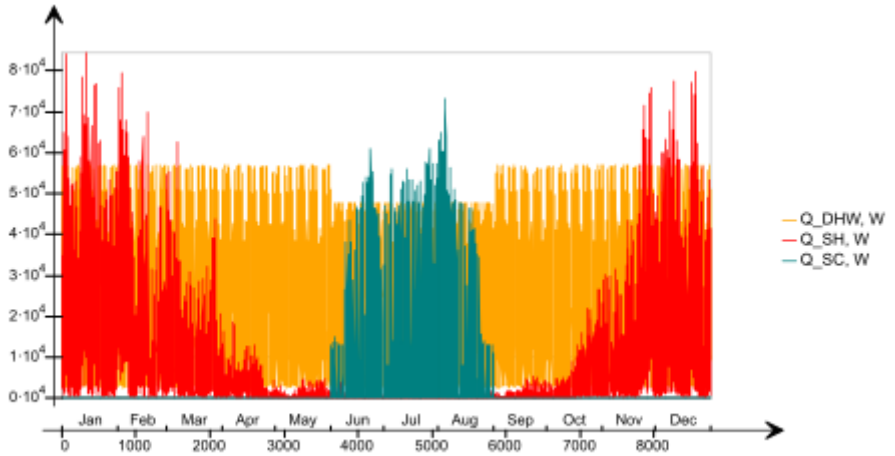

Figure 7: Time series of space (red) and domestic hot water (orange) heating demand, and space cooling (teal) demand over one year

Space heating peak demand has been simulated according to the climate region,

with an external temperature of -26°C. The peak request is 87 kW. Domestic hot water peak results in 58 kW.
Cooling peak load equals to 65 kW and occurs in July.

2.2 Office building demand

The office building will be located in the north-western part of the plot. It comprises office spaces, a restaurant for the employees and some laboratory facilities.
Based on the preliminary architect's drawings, the office has a net heated area of 20600 m^2 (24900 m^2 gross area) and a volume of approximately 111557 m^2. Figure 8 shows the mass-like shape of the planned office building.

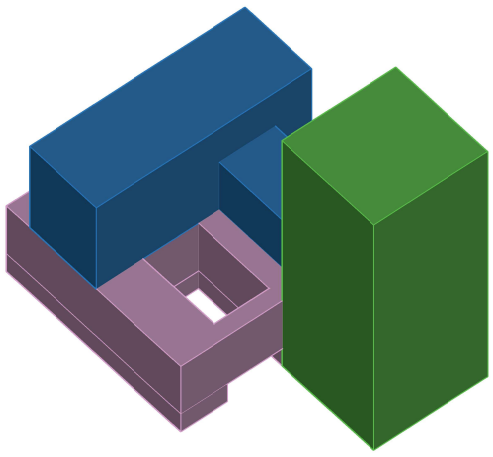

Figure 8: Schematic mass representation of the office building

The information available is not enough to perform a dynamic energy simulation as in the apartment building case. The approach for defining the energy demand is based on the preliminary drawings (gross and net areas, facade area, floor heights), standard values from the regulations and research approximations.

Heating and cooling demand are determined based on data provided on the study [9], where the energy consumption of different building types were evaluated. Energy consumption is evaluated considering different building construction years. The category that has characteristics matching the current regulation is D1. The figures presented are calculated through dynamic energy simulation carried out with IDA ICE and with using as weather data the test reference year 2012 of Jyväskylä, being this city the reference used for Finnish building's energy consumption comparisons.

Based on these figures, the space heating energy is assumed to be 41 kWh/m^2a, therefore the total space heating demand (Q_{SH}) is:

$$Q_{SH} = 20600m^2 \cdot 41\frac{kWh}{m^2} = 844600\frac{kWh}{a} = 844.6\frac{MWh}{a} \tag{2.1}$$

The mass of water that needs to be heated results:

$$m_{DHW} = V_{lkv,omin} \cdot A_{gross} \cdot \rho_w \tag{2.2}$$
$$= \frac{100\ l/brm^2a}{1000\ m^3} \cdot 24900\ m^2 \cdot 1000\frac{kg}{m^3} = 2490000\frac{kg}{a}$$

where $V_{lkv,omin} = 100\ l/brm^2a$ is the annual water volume usage per gross floor area, $A_{gross}\ [m^2]$ is the gross floor area of the building and $\rho_w\ [m^3]$ is the water density.

The heating energy needed (Q_{DHW}) is:

$$Q_{DHW} = m_{DHW} \cdot c_{p,w} \cdot (T_{DHW,supply} - T_{DHW,inlet}) \tag{2.3}$$
$$= 2490000\frac{kg}{a} \cdot 4,2\frac{kJ}{kgK} \cdot (58-10)°C \cdot \frac{1}{3600kJ/kWh} = 139440\frac{kWh}{a}$$

where $m_{DHW}\ [kg/a]$ is the required water mass, $c_{p,w}\ [kJ/kgK]$ is the specific heat of water, $T_{DHW,supply} = 58°C$ is the water supply temperature and $T_{DHW,inlet} = 10°C$ is the cold water temperature.

The estimation of the cooling demand follows the approach used for space heating. With a specific cooling demand of 16 kWh/m^2, the total space cooling energy (Q_{SC}) required results:

$$Q_{SC} = 20600m^2 \cdot 16\frac{kWh}{m^2} = 329600\frac{kWh}{a} = 329.6\frac{MWh}{a} \tag{2.4}$$

2.2.1 Office building load profiles

The hourly profiles are based on the VTT study [9]. From the model building's figures, specific hourly values per square meter are obtained and then scaled on the actual area of the office under investigation.

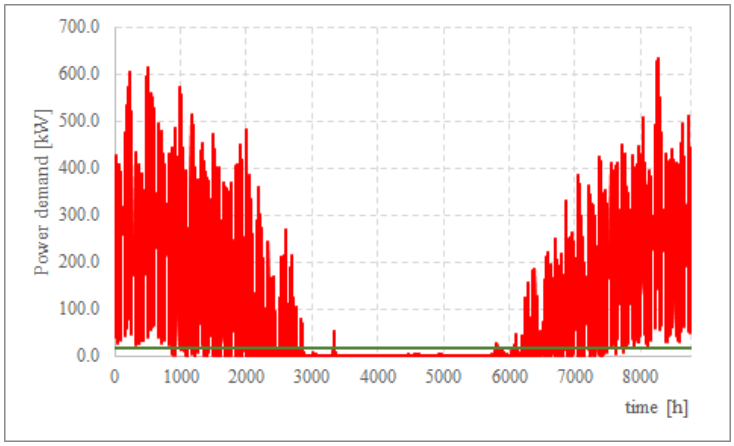

(a) Space heating (red) and domestic hot water (green) energy demand

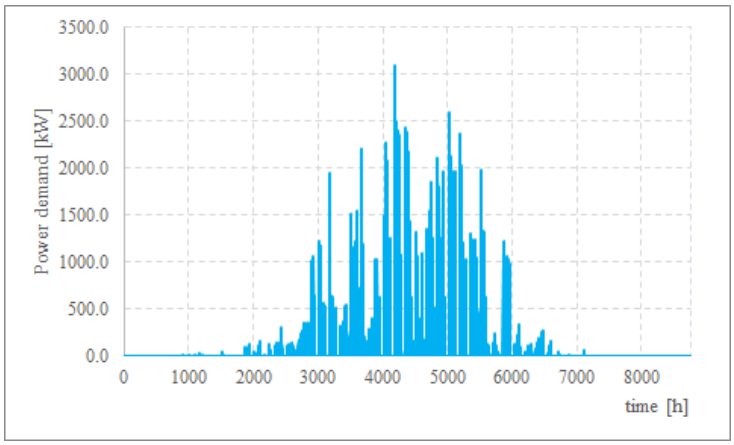

(b) Space cooling energy demand for office building

Figure 9: Net energy demands for office building

2.3 Total site demand

The total energy demand of the plot corresponds to the sum of residential and office buildings demands. On the residential part total demand, even though in reality some variations in the energy consumption are present in different buildings, here it was assumed they all have the same energy demand per square meter, which is derived from the model building simulation.

Table 3: Specific energy demand for model apartment building

Heating (DH)	55.4 kWh/m^2a
Cooling (DC)	4.4 kWh/m^2a

Table 4: Dimensioning power for apartment buildings

Space heating	19 W/m^2
DHW	13 W/m^2
Total	32 W/m^2
Space cooling	14 W/m^2

Scaling these values on the total residential area, the overall site energy consumption is obtained. Heating energy demand is 5038.1 MWh/a, consisting in 1357.6 MWh/a for SH and 3680.5 MWh/a for DHW; total cooling energy demand is 400.7 MWh/a.
The same approach is used on the load profiles, so that the hourly variation is also known for the entire residential part.

Figure 10 shows the monthly energy demand of both residential and office building. Domestic hot water represents a big share of the heating demand, since it is needed

throughout the year and is not weather dependent. The biggest share of the demand for domestic hot water comes from the apartment buildings. Residential buildings require cooling only during the hottest months, while for the office building there is the need for simultaneous heating and cooling.

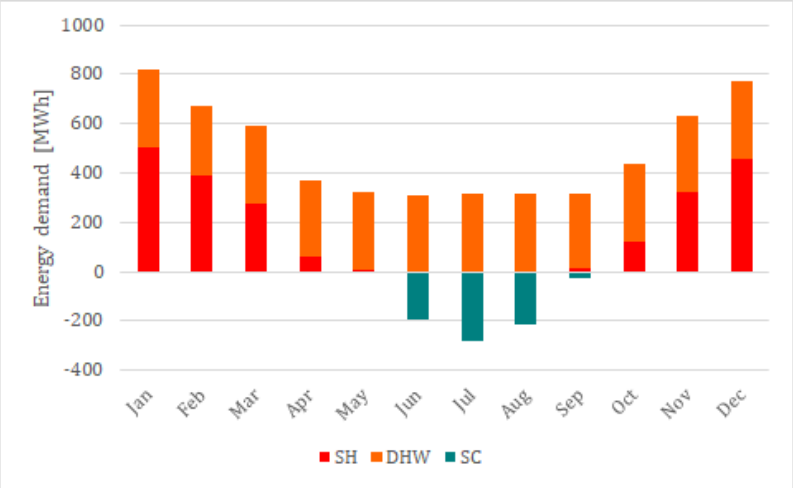

Figure 10: Monthly energy demand for the whole plot

Total figures for the area result in a heating demand of 6022 MWh/a, of which 1497 MWh/a for space heating and 4525 MWh/a for domestic hot water, and in a cooling demand of 730 MWh/a.

The peak loads for the block of flats are calculated from Table 4, resulting in 1727 kW, 1182 kW and 1273 kW for space heating, domestic hot water and space cooling respectively. Peak loads for the office building are instead estimated from its load profiles.

Therefore, the area would require at design conditions, 2.36 MW for heating and 4.37 MW for cooling.

3 Geothermal systems

Geothermal energy is the energy stored under Earth's surface in form of heat. On the surface, the thermal energy comes mainly from solar radiation, while in deeper layers it comes from the decomposition of radioactive materials [10].

Geothermal energy presents many advantages. It is a renewable energy source, independent of seasonal changes and weather effects, including climate change, it is capable of providing the baseload power, it is compatible with centralised and distributed energy generation, it is globally available, especially for direct use. Geothermal energy can be used to produce electricity, extract/reject or store heat in the ground.

In 2018, geothermal electricity total installed capacity all over Europe was up to 3,091 MWe, which corresponds to 127 operative power plants. The use of deep geothermal for heating and cooling has also grown, with 12 new or renovated plants, for a total capacity of 149 MWth. Lastly, shallow geothermal systems (ground source heat pumps - GSHP, underground thermal energy storage - UTES) have seen a constant growth, which brought the installed capacity to 23000 MWth corresponding to 1,9 million GSHP installations.

Direct use of geothermal has been known for centuries, since middle Paleolithic, when natural hot springs were already used for bathing. The first industrial utilisation of geothermal energy took place in Larderello, Italy, where boric acid was harnessed from the hot groundwater present in the area. Here, in 1904, occurred also the first electricity generation and in 1913 the first 250 kW commercial power unit was installed. Other countries started then to develop their geothermal systems. In 1928, Iceland began exploiting its geothermal resource for both heating and electricity production, making it nowadays the principal source for energy generation (represents 29% of electricity production and covers 90% of heating demand).

Depending on the depth at which the resource is harnessed, one can distinguish between two categories of geothermal energy: shallow and deep.

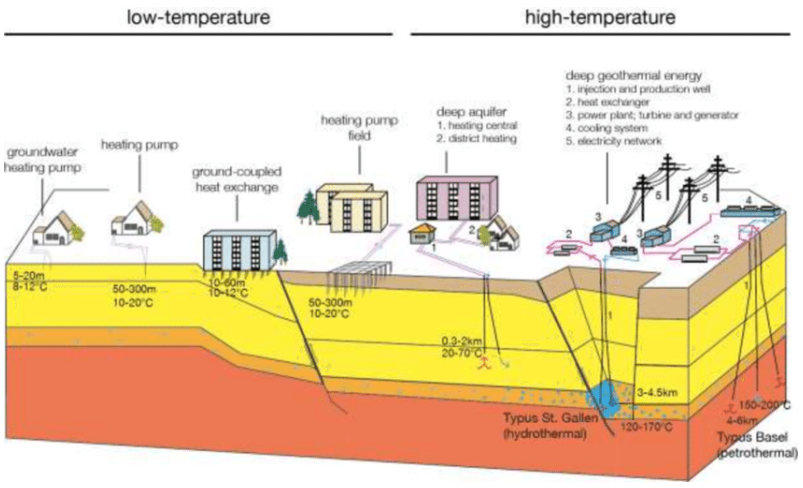

Figure 11: Different uses of geothermal energy [11]

Shallow geothermal energy, when heat is collected near the surface; typically, the term shallow applies to depths up to 400 m. Deep geothermal energy refers to the depths below 400 m. Depth influences the available temperatures in the ground and, therefore, the possibilities of utilising geothermal energy: shallow geothermal is used for heating/cooling production while deep geothermal can be used also for electricity generation.

Direct use of geothermal energy includes swimming pools and spas, space heating and cooling, district heating, agricultural (e.g. greenhouse heating) and industrial (utilization of either steam or water, e.g. in drying process) applications and geothermal heat pumps.

Geothermal, or ground source, heat pumps utilize the heat contained in the uppermost 400 m of the ground. The heat pump is used to increase or decrease, depending on the season, the temperature levels which are coming naturally from the ground. It is a highly versatile system, making its installation possible from small, one-family houses, to complexes of buildings, offices, schools, etc.

3.1 Shallow geothermal systems

A GHSP system comprises three main elements: the building side, the heat pump(s) and the ground circuit.

Several systems for the ground coupling are available and they can be divided into two main categories:

- Open-loop systems: there is a direct use of groundwater through wells.
- Closed-loop systems: the heat is harnessed by circulating a fluid (water-antifreeze solution) inside a heat exchanger inserted in the ground. They can be horizontal, vertical, structures, etc.

Table 5 summarises the different methods to collect heat from the ground in shallow geothermal systems.

Table 5: Shallow geothermal heat exchangers

Horizontal ground heat exchangers	1.2-2.0 m depth (horizontal loops)
Borehole heat exchangers	10-250 m depth (vertical loops)
Energy piles	5-45 m depth
Ground water wells	4->50 m depth
Water from mines and tunnels	

Open-loop systems use water directly as a heat source, coming either from the ground or a lake. It is circulated through a heat exchanger and then discharged back to the ground through a second well or to the lake.

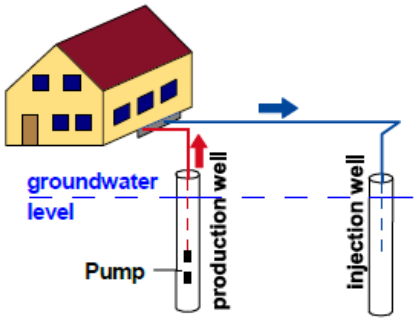

Figure 12: Schematic of an open-loop system

A closed horizontal loop consists of plastic pipes placed close to the ground surface: typically, pipes are buried 1 to 2 m under the surface with 1 m spacing between the pipes. They can be connected in series or parallel. Variants to this configuration consist in trench collectors or a more compact system called "slinky".

These systems are less efficient than vertical loops, due to the lower temperatures available, they are more influenced by air temperature variations and they require a significantly wider area for installation. The highest efficiency is obtained in fine-grained soils with a high content of water (e.g. clay). The ground heat is recharged in this case mainly through solar radiation.

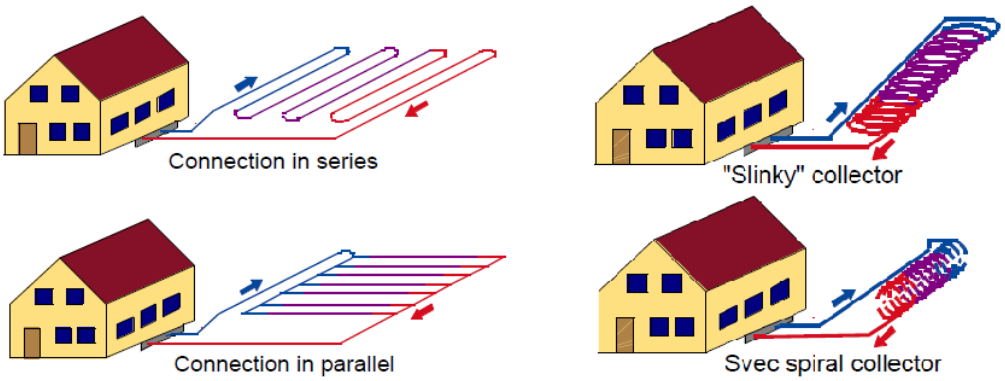

Figure 13: Horizontal closed loop collectors

Closed vertical loops consist of a borehole (BH) in which is inserted a borehole heat exchanger (BHE). If foundation piles are used, energy piles can be also an option to have a ground heat exchanger. These systems can be used in both heating and cooling mode, collecting heat in winter and rejecting the excess heat to the ground during summer. High efficiencies are reached when the boreholes are installed in rocks with a high content of silica (granite, gneiss).

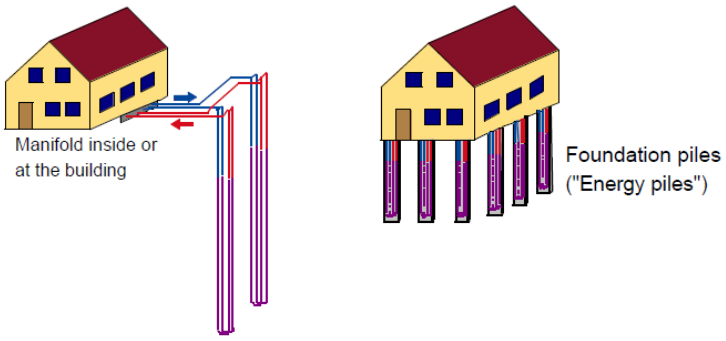

Figure 14: Vertical closed loop collectors

Shallow geothermal installations can be used for only heating/cooling purposes or as Underground Thermal Energy Storage (UTES), when used to store seasonally heat underground by increasing the ground temperature. Anyway, the difference between these two applications is quite thin, becoming even more uncertain in large installations.

3.2 Borehole heat exchangers

A borehole heat exchanger consists of a certain pipe arrangement inserted inside the borehole drilled in the ground. There are mainly two types of borehole heat exchanger (BHE):

- U-pipes (single or multiple): a pair of pipes connected with a U-shaped turn at the bottom. One borehole can contain single, double or triple U-pipe. The heat carrier fluid is circulated inside the pipe.
- Coaxial pipes: two pipes of different diameter inserted one inside the other; the fluid is pumped downwards in the outer channel and collected back to the surface through the smaller channel.

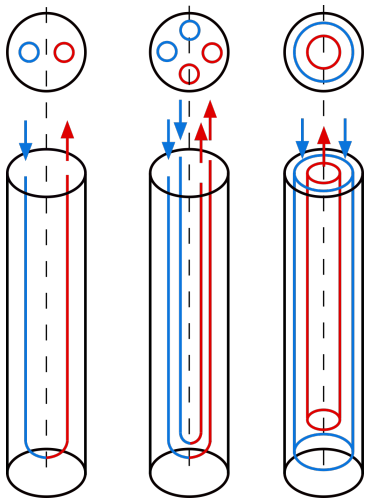

Figure 15: Borehole heat exchangers: single U-pipe, double U-pipe and coaxial pipes

The boreholes installed in Central Europe are generally grouted, with e.g. bentonite, concrete or thermally enhanced grouts, to ensure better contact and enhance heat transfer. In Scandinavian countries, the boreholes are typically groundwater-filled.

Extracting heat during winter causes the ground to cool down locally. The design must take into account this phenomenon and the heat regeneration time in the ground. In the case of a single borehole, e.g. used in a single-family house, the heat can be restored during the summer season. When several boreholes are present, the effect becomes much more important. The design must include defining the appropriate number of boreholes, their length and spacing to avoid excess cooling in the ground and having, in the long run, a system which is inefficient. This effects are mitigated if, during the cooling season, heat is rejected to the ground.

Among the different types of ground heat exchangers, this work will focus on the borehole heat exchangers with single U-pipe. The working principle and the thermal behaviour of a single borehole are described. Mathematical formulations which define one of the most important parameters in the borehole thermal behaviour, the borehole thermal resistance, are also presented. Shortly, the methods used to model the behaviour of a borehole field are summarised and design considerations are briefly discussed.

The heat carrier fluid is circulated through the U-pipe installed in the borehole, collecting heat from the ground and conveying it back to the heat pump. After the evaporator, the fluid becomes colder and the loop can start again. The hole gets colder, making the heat flow from the surrounding ground towards it.

The heat transfer inside the ground takes place mostly through pure conduction. Radiation is neglected, but when the borehole is filled with groundwater, the heat transfer occurs also through convection. This phenomenon is much more complex than conduction, since it is related to fluid and soil properties, porosity, hydraulic properties, etc. requiring a simulation software to be analysed.

Despite its low thermal conductivity, the use of water instead of other grouts can be advantageous. The natural convection occurring in the groundwater enhances heat transfer, making the heat to flow more easily into the heat exchanger. Measured resistances in groundwater-filled borehole in Sweden show that the resistance is actually lower than a grouted borehole. Thermal response tests (TRT) performed in a borehole at a campus of Luleå University of Technology, containing two separate U-pipes DN40PN6, registered borehole thermal resistances as low as 0.059-0.065 Km/W [12]. In Göteborg, a TRT on a system of 9 boreholes measured resistances of 0.05-0.07 Km/W [13].

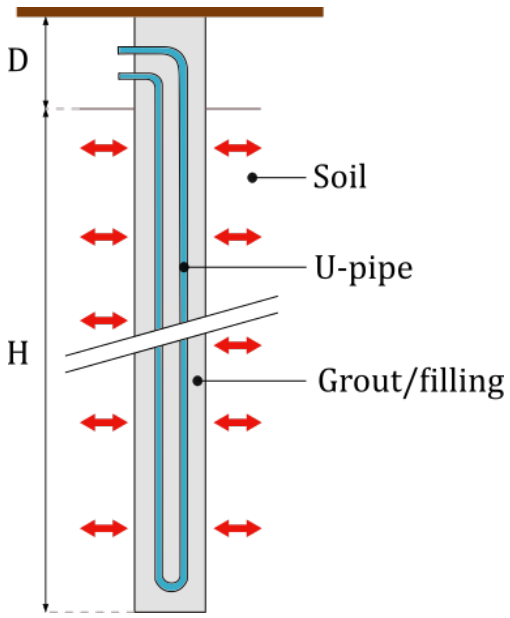

Figure 16: Schematic of a grouted borehole heat exchanger with single U-pipe. D is the length of the casing or level of ground water. H is the active length of the borehole.

The BH has an active length (H) where the heat transfer occurs. The depth D is assumed to be thermally insulated and can correspond to the length of the casing or the level of groundwater. Figure 16 illustrates schematically the main characteristics and components of a grouted BHE with a single U-pipe. The ground is often non-homogeneous, with a top layer with lower thermal conductivity. Its effect on the overall thermal performance is less than 2%, therefore the influence of a top layer up to 10 m deep can be neglected [14]. There are several factors affecting the borehole heat exchanger performance. According to Eskilson [14], for a single BHE three important parameters are:

1. *Thermal conductivity of the ground:* according to Fourier's law, heat conduction is directly proportional to the thermal conductivity. Therefore, a higher thermal conductivity is preferred to have a higher heat transfer, such as in solid rocks containing quartz.

2. *Borehole thermal resistance:* it is the resistance between the heat carrier fluid and the borehole wall. It is one of the most important parameters in the borehole thermal behaviour, since it can be designed and controlled, unlike the resistance of the ground. It is desirable to have a resistance as low as possible.

3. *Undisturbed ground temperature (average):* it is the average temperature in the ground over the borehole depth. The heat extraction depends on the available temperature drop between this undisturbed ground temperature and the heat carrier fluid temperature. The bigger the available temperature drop, the more heat transfer is obtainable.

3.3 Borehole thermal resistance

The heat transfer to the heat exchanger is greatly affected by the borehole thermal resistance. It represents the fluid-to-ground thermal resistance being, therefore, a measure of how effectively the heat can be transferred between the heat carrier fluid and the ground. It depends upon several parameters, comprising thermal and geometric properties of all the materials and components present in the borehole. The resistances associated with every part can be assembled into a single resistance, R_b, reducing to one the parameters which describe the thermal process in the borehole. The general relation for the heat transfer between heat carrier fluid and ground is:

$$T_f - T_b = q \cdot R_b \tag{3.1}$$

where,

T_f is the local mean fluid temperature, °C

T_b is the temperature at the borehole wall, °C

q is the heat transfer rate per unit length, W/m

R_b is the borehole (fluid-to-ground) thermal resistance, mK/W

This resistance has only a local value, thus it would be more accurate to define an effective borehole thermal resistance, which is going to be described in section 3.3.3.

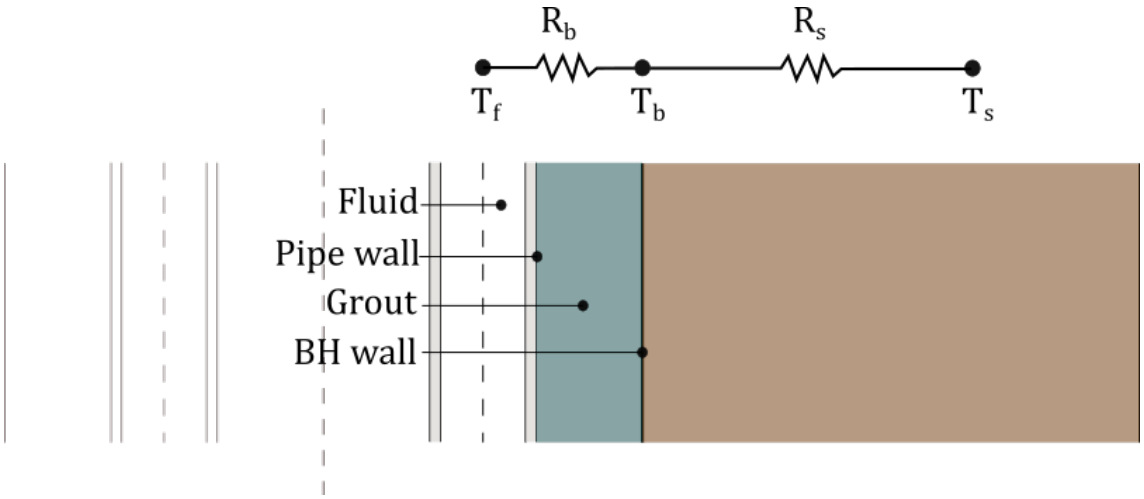

Figure 17: Scheme of thermal resistances: R_b and R_s are, respectively, the borehole and the ground resistance

Figure 17 shows that the borehole thermal resistance is a function of the heat transfer that occurs between the fluid and the borehole wall. Three main components can be recognised:

1. convective heat transfer inside the pipes, R_{fc}

2. conductive heat transfer through the pipe walls, R'_p
3. conductive heat transfer through the grout/filling material, R_g

All the thermal properties of the materials are thus important, to minimise the overall resistance. The problem cannot be reduced to the simple computing of these three heat transfer components, since other phenomena that influence the thermal resistance occur and need to be taken into account. Temperature gradient in the bedrock, the temperature difference between the channels, which also depends on the flow rate velocity (lower velocities increase the temperature difference), their reciprocal interaction (short-circuiting), their arrangement inside the borehole (shank spacing), are all elements that complicate the definition of the thermal resistance. Moreover, if the borehole is groundwater-filled, the effects due to water natural convection need to be taken into account. Deriving analytical solution is simple in the case of a single duct, while becomes complicated when considering multiple ducts in a composite region (U-pipe) [15].
The case of a single duct equals a simple pipe, for which a resistance R_p is derived. As a general definition, total fluid-to-ground thermal resistance R_b can be treated as a sum of resistances in series. It will be a combination of two parts: the grout thermal resistance R_g and the pipe thermal resistance R_p.

$$R_b = R_g + \frac{R_p}{N} \tag{3.2}$$

where N is 2 for single, 4 for double and 6 for triple U-pipes.

In reality, calculating the borehole thermal resistance is more complex. Typically, the calculation methods are based on the assumption that a two-dimensional steady-state heat transfer takes place locally at each depth z and time t. The solution is therefore found by solving this heat conduction problem in the plane perpendicular to the pipes. The pipes are considered to be inside a circular region (borehole) surrounded by an infinite region with a different thermal conductivity (ground).

The thermal behaviour of the borehole can be analysed by considering a heat flow circuit, which represents the relation between temperatures and heat flows. The case of two pipes (U-pipe) is represented with a Δ thermal circuit, with resistances between the temperature nodes in the pipes and at the borehole wall. Its graphical representation is shown in Figure 18.

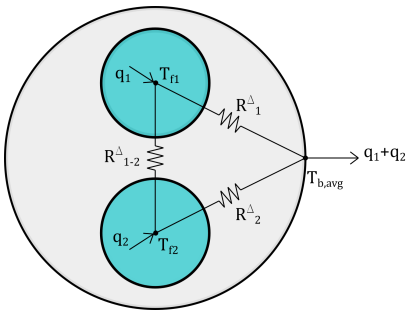

Figure 18: Borehole with U-pipe and equivalent delta thermal circuit

The Δ circuit is based on the following relations:

$$q_1 = \frac{T_{f1} - T_{b,avg}}{R_1^{\Delta}} + \frac{T_{f1} - T_{f2}}{R_{12}^{\Delta}} \tag{3.3}$$

$$q_2 = \frac{T_{f2} - T_{b,avg}}{R_2^{\Delta}} + \frac{T_{f2} - T_{f1}}{R_{12}^{\Delta}} \tag{3.4}$$

where q_i $[W/m]$ is the heat flux and $T_{f,i}$ $[^{\circ}C]$ is the fluid temperature in pipe i, R_1^{Δ} and R_2^{Δ} [mK/W] are the resistances between the fluid and the ground, R_{12}^{Δ} is a mathematical artefact, due to the chosen network representation.
These resistances include the resistance of fluid and pipe. The total borehole resistance is obtained by setting $T_{f1} = T_{f2} = T_f$ and solving for two parallel resistances R_1^{Δ} and R_2^{Δ}

$$R_b = \frac{R_1^{\Delta} R_2^{\Delta}}{R_1^{\Delta} + R_2^{\Delta}} \tag{3.5}$$

Moreover, it is possible to define the total internal resistance between the two channels of the U-pipe (R_a).

$$R_a = \frac{R_{12}^{\Delta}(R_1^{\Delta} + R_2^{\Delta})}{R_{12}^{\Delta} + R_1^{\Delta} + R_2^{\Delta}} \tag{3.6}$$

This resistance is important in considering the short circuiting and to calculate the effective borehole thermal resistance.

3.3.1 Pipe thermal resistance

The pipe thermal resistance is composed of two parts: the convective resistance of the heat carrier fluid and the conductive resistance at the pipe wall.

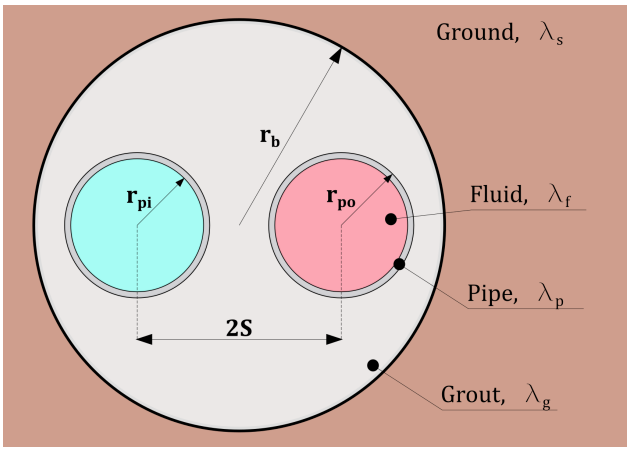

Figure 19: Principal dimensions are the inner (r_{pi}) and outer (r_{po}) pipe radii, the borehole radius (r_b), 2S is the shank spacing. The figure indicates also the main components and their respective thermal conductivities (λ_i)

The convective resistance component (R_{fc}) is given by:

$$R_{fc} = \frac{1}{2\pi r_{pi} h} \tag{3.7}$$

where h $[W/m^2K]$ is the heat transfer coefficient, calculated on the basis of the Nusselt number (Nu).

$$h = \frac{\lambda_f Nu}{D} \tag{3.8}$$

$$Nu = \frac{(\frac{f}{8})(Re - 1000)Pr}{1 + 12.7\frac{f}{8}^{0.5}(Pr^{\frac{2}{3}-1})} \tag{3.9}$$

$$f = [0.79ln(Re) - 1.64]^{-2} \tag{3.10}$$

$$Re = \frac{\rho v D}{\mu} \tag{3.11}$$

$$Pr = \frac{\mu c_p}{\lambda_f} \tag{3.12}$$

where

D is the characteristic length, which coincide in this case with the internal pipe diameter

f is the friction factor

Re is Reynolds number: a transient-turbulent flow (Re>2300) is required for efficient heat transfer.

Pr is Prandtl number.

λ_f is the fluid thermal conductivity, W/mK

ρ is the fluid density, kg/m^3

v is the fluid velocity, m/s

μ is the fluid viscosity, kg/ms

c_p is the fluid specific heat capacity, J/kgK

The conductive resistance (R'_p) is given by:

$$R'_p = \frac{1}{2\pi\lambda_p} \ln \frac{r_{po}}{r_{pi}} \tag{3.13}$$

The total pipe resistance (R_p) is then:

$$R_p = R_{fc} + R'_p \tag{3.14}$$

3.3.2 Grouted borehole thermal resistance

The pipe-to-borehole thermal resistance, also known as grout thermal resistance, represents the thermal resistance between the outer wall of the pipes and the outer wall of the borehole. Some of the methods available for calculating this resistance are presented here.

The equivalent radius method considers the two branches of the U-pipe as one, which radius is the equivalent radius (r_{eq}), and the heat transfer is then simplified as a conduction between one pipe and the borehole wall.

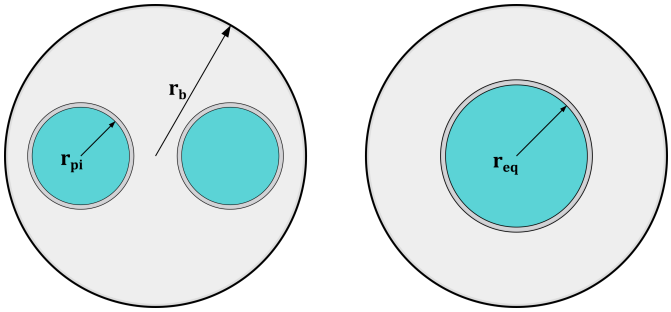

Figure 20: Equivalent radius geometry

$$R_b = R_g = \frac{1}{2\pi\lambda_g} ln\left(\frac{r_b}{r_{eq}}\right) \tag{3.15}$$

This approximation does not take into account the short-circuiting between the two channels. Another formulation, derived from the previous one by Gu and O'Neal [16], includes instead the shank spacing (2S).

$$R_b = R_g = \frac{1}{2\pi\lambda_g} ln\left(\frac{r_b}{r_{eq}}\sqrt{\frac{r_{po}}{S}}\right) \tag{3.16}$$

More detailed consideration of the shank spacing effect has been investigated by Paul [17], which derived an empirical formula and coefficients that include three possible configurations of the shank spacing.

$$R_b = \frac{1}{\beta_0 \left(\frac{r_b}{r_{po}}\right)^{\beta_1} \lambda_g} \tag{3.17}$$

where the coefficients are:

Table 6: Coefficients for different shank configurations

Configuration	β_0	β_0
A	20.10	-0.9447
B	17.44	-0.6052
C	21.91	-0.3796

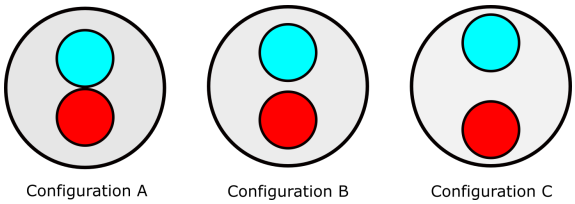

Figure 21: Pipe configurations

Another empirical estimation of the pipe-to-borehole resistance has been proposed by Sharqway et al. [18] as:

$$R_g = \frac{1}{2\pi\lambda_g}\left[-1.49\frac{S}{d_b} + 0.065ln\frac{d_b}{d_{po}} + 0.436\right] \tag{3.18}$$

where S is half of the shank spacing [m], λ_g is the grout thermal conductivity [W/mK], d_b is the borehole diameter [m] and d_{po} is the pipe external diameter[m].

A greater level of accuracy can be achieved through methods that derive an analytical expression directly for the overall borehole thermal resistance. Hellström [15] derived an analytical solution for the borehole thermal resistance based on the infinite line source theory. The flow channels are modelled as infinite pipes with similar fluid temperatures and heat fluxes. His solution, for single U-pipe, is:

$$R_b = \frac{1}{4\pi\lambda_g}\left[\beta + \ln\frac{r_b}{r_p} + \ln\frac{r_b}{S} + \sigma\ln\frac{r_b^5}{r_b^4 - \left(\frac{S}{2}\right)^4}\right] \tag{3.19}$$

where β and σ are expressed as:

$$\beta = 2\pi\lambda_g R_p \tag{3.20}$$

$$\sigma = \frac{\lambda_g - \lambda_s}{\lambda_g + \lambda_s} \tag{3.21}$$

where λ_g and λ_s are the grout and ground thermal conductivity.
Another approach is the multipole method. It was first developed by Bennet et al. [19] in 1987 and later revised by Hellström in 2006 [20].

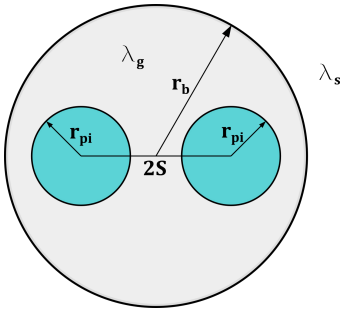

Figure 22: Geometry for multipole method [15]

This method solves the two-dimensional steady-state heat transfer for any number of arbitrarily placed pipes in a composite region. It uses a combination of line sources and multipoles. The solution of a first-order multipole, for a single U-pipe, with symmetrically placed shanks, is:

$$R_b = \frac{1}{4\pi\lambda_g}\left[\beta + \ln\frac{r_b}{r_p} + \ln\frac{r_b}{S} + \sigma\ln\frac{r_b^5}{r_b^4 - \left(\frac{S}{2}\right)^4}\right] - \frac{1}{2\pi\lambda_g}\frac{\frac{r_{po}^2}{D^2}\left[1-\sigma\frac{4S^4}{(16r_b^4-S^4)}\right]^2}{\left\{\frac{1+\beta}{1-\beta} + \frac{r_p^2}{S^2}\left[1+\sigma\frac{r_b^4 S^4}{(r_b^4-\left(\frac{S^2}{2}\right)^4)^2}\right]\right\}} \tag{3.22}$$

The first term in the equation is exactly the line source solution, while the second addend derives from the first-order multipole approximation.

3.3.3 Effective borehole thermal resistance

Equation (3.1) describes the heat transfer at a given depth and has only a local value. Moreover, the different temperatures that the heat carrier fluid has in the two channels, cause the heat transfer to take place between the pipes, especially at low flow rates, (reducing significantly the BH efficiency) increasing the BH resistance. This phenomenon is known as short-circuit. When defining an effective borehole thermal resistance, one obtains a relation which is not only valid throughout the whole borehole length, but also includes the short-circuiting phenomenon.
The general formulation of heat transfer is similar to the one presented in Equation (3.1) but, in this case, a fluid temperature which is equal to the simple average of inlet and outlet temperatures and an average borehole wall temperature are used.

$$R_b^* = \frac{\bar{T}_f - \bar{T}_b}{q} \tag{3.23}$$

where R_b^* is the effective borehole thermal resistance [mK/W], $\bar{T}_f$ is the average of inlet and outlet fluid temperature [$^\circ C$], $\bar{T}_b$ is the average borehole wall temperature and q is the heat transfer rate per unit length [W/m].
It is possible to derive an analytical expression for this resistance when considering simplified boundary conditions. For the case of single U-pipe, Hellström derived the effective resistance considering two extreme conditions: uniform borehole wall temperature (UBW) and uniform heat flux along the borehole (UHF) [15]. The effective borehole resistance can be calculated as the arithmetic mean of these two cases.

$$(UBW) \quad R_b^* \approx R_b + \frac{1}{3}\frac{1}{R_{12}^{\Delta}}\left(\frac{H}{C_f V_f}\right)^2 + \frac{1}{12}\frac{1}{R_b}\left(\frac{H}{C_f V_f}\right)^2 \tag{3.24}$$

$$(UHF) \quad R_b^* = R_b + \frac{1}{3}\frac{1}{R_a}\left(\frac{H}{C_f V_f}\right)^2 \tag{3.25}$$

where C_f is the specific heat of the heat carrier fluid, V_f is the mass flow rate of the heat carrier fluid, R_a, R_1^{Δ} $and R_{12}^{\Delta}$ are intermediate resistances, calculated as follows [20]:

$$R_a = \frac{1}{\pi\lambda_b}\left[\beta + \ln\left(\frac{2S}{r_p}\right) + \sigma\ln\left(\frac{r_b^2+S^2}{r_b^2-S^2}\right)\right] - \frac{1}{\pi\lambda_g}\left\{\frac{\frac{r_p^2}{4S^2}\left[1+\sigma\frac{4r_b^4S^2}{(r_b^4-S^2)}\right]^2}{\left[\frac{1+\beta}{1-\beta} - \frac{r_p^2}{4S^2} + \sigma\frac{2r_p^2r_b^2(r_b^4+S^2)}{(r_b^4-S^2)^2}\right]}\right\} \quad (3.26)$$

$$R_1^{\Delta} = \frac{1}{2\pi\lambda_b}\left[\beta + \ln\left(\frac{r_b}{r_p}\right) + \ln\left(\frac{r_b}{2S}\right) + \sigma\ln\left(\frac{r_b^4}{r_b^4-S^4}\right)\right] - \frac{1}{2\pi\lambda_b}\frac{\frac{r_p^2}{4S^2}\left[1-\sigma\frac{4S^4}{(r_b^4-S^4)}\right]^2}{\left\{\frac{1+\beta}{1-\beta} - \frac{r_p^2}{4S^2}\left[1+\sigma\frac{16r_b^4S^4}{(r_b^4-S^2)^2}\right]\right\}} \quad (3.27)$$

$$R_{12}^{\Delta} = \frac{R_aR_b}{R_b - 0.25R_a} \quad (3.28)$$

where r_p is the U-pipe outer radius, S is half of the distance between pipes' centers, λ_b is the grout conductivity.

The multipole method is regarded as the most accurate since it provides an exact algorithm to compute the steady-state borehole thermal resistance [21]. Therefore, it has been implemented in simulation software for GSHP design, such as EED [22] and GHLEPRO.

3.4 Ground interaction

When designing a borehole field, the long-term performance is a key factor to be analysed. The field performance is affected by number, configuration and position of boreholes, as well as the heat extraction/injection rates, which create a thermal disturbance in the ground temperature.

The borehole thermal response is not only a function of the thermal process in the borehole, but also of the heat transfer between its wall and the ground. Once again, the heat flux can be represented through resistances, R_b and R_s respectively, and temperature nodes. Resistances are in series and their combination gives the overall thermal resistance (R_t):

$$R_t = R_b + R_s \quad (3.29)$$

A typical approach is to calculate the required borehole length by analysing the system long-term performance. Several methods exist for the modelling of the heat transfer in the ground outside the boreholes. Models can analyse either the long term or the short term response. They can be analytical, numerical or models

which combine these two approaches. Analytical methods are preferred in practical applications, because of shorter computational times and ease of parametric design implementation. Numerical methods, despite their longer computational time, are superior in terms of accuracy of the solution.

The Infinite Line Source (Kelvin's line source) is an analytical method which models the borehole as a line source of infinite length and constant heat flux, surrounded by a homogeneous medium. This method assumes an initial uniform ground temperature and neglects axial heat transfer, making this a one-dimensional model. The solution is found solving the radial heat transfer in a plane perpendicular to the line source. Another analytical method is the Infinite Cylindrical Source, in which the borehole is modelled as a cylinder (representing the borehole wall). The ground is assumed to have constant properties and the GHE a constant heat flux. The solution is again found for radial transient heat transfer, which takes place only by pure conduction. Must be mentioned that both models ignore the end effects of its heat source by considering the line or cylinder infinite.

A numerical method, Finite Line Source, has been developed by Eskilson in his PhD thesis. He modelled the thermal behaviour of the borehole using non-dimensional thermal response functions, the g-functions. The model is based on the superposition of the different numerical solution obtained for each borehole. The g-functions contain the whole information about the thermal influence between boreholes and they are used for the numerical modelling of the thermal response of a specific borehole field. They are a function of geometrical dimensionless parameters and a dimensionless time step.

$$T_b = T_s - \frac{q(t)}{2\pi\lambda_s} \cdot g\left(\frac{t}{t_s}, \frac{r_b}{H}, \frac{B}{H}\right) \tag{3.30}$$

where

$\frac{t}{t_s}$ is the dimensionless time step

$\frac{r_b}{H}$ is the dimensionless borehole radius

$\frac{B}{H}$ is the field aspect ratio, between borehole distance and borehole length

Eskilson built a computer program which calculates the g-functions for different borehole configurations: one g-function characterises only and only one borehole field, for certain values of the geometrical dimensionless parameters. The model follows the evolution of the temperatures along time and is the only model which gives a very precise estimation of the long-term influence between boreholes [23].

From this model, a hybrid approach can be derived. The g-functions can be calculated for several borehole configurations, spacing and depths, and stored in a database, which can then be implemented in building energy simulation software, reducing the normal computational time of numerical models. This approach is utilised in many simulation software, such as EED, TRNSYS, Energy Plus and GLEHPRO.

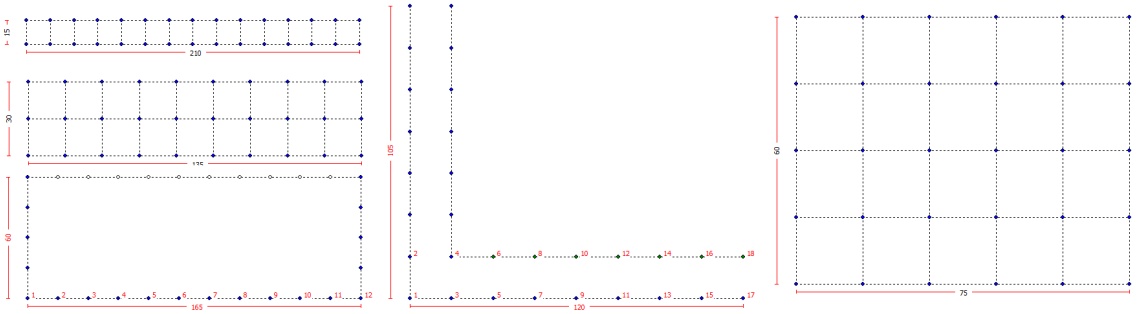

Figure 23: Examples of possible configurations for 30 boreholes (Source: Earth Energy Designer)

3.5 Borehole fields

In the following, some measures regarding the design of a large borehole field are presented, (concerning both geometrical factors and hydraulics).
The designer should focus on the overall system performance, thus the system BH field and heat pump(s) must be considered together and optimised.

The aim is to define appropriate boundaries for the system for its whole design life: this means defining fluid temperatures and heat pump efficiency range, since lower fluid temperatures result in decreased COP to an unacceptable level. Therefore, the ground-loop must be designed to match these criteria, during the life cycle and under extreme (peak load) conditions.

The ground loop should have an appropriate length to fulfil the heating and cooling demands, under both base and peak load conditions. It should have also a sufficiently low thermal resistance and hydraulic losses, in order to minimise the pumping power.

A first impact on the system performance can be achieved at borehole level, by minimising its thermal resistance. Four main factors can be identified.

- Material's thermal conductivity: as previously discussed, the higher the thermal conductivity, the lower the thermal resistance. Despite copper or steel have higher thermal conductivities, HDPE is preferred as pipe material because of lower costs and higher resistance to corrosion.

  The other thermal conductivity which can be controlled is the grout one. Nowadays, thermally enhanced grouts (with high quartz contents) have been developed, with higher conductivities than traditional bentonite fillings, which also have a tendency to shrink away from the pipes. Saturated gravel shows the lowest BH resistance among all the possible fillings.

- Pipe diameter and number: BH resistance is lower when using a 40 mm pipe compared to a 32 mm. Even lower resistances can be achieved with double U-pipes.

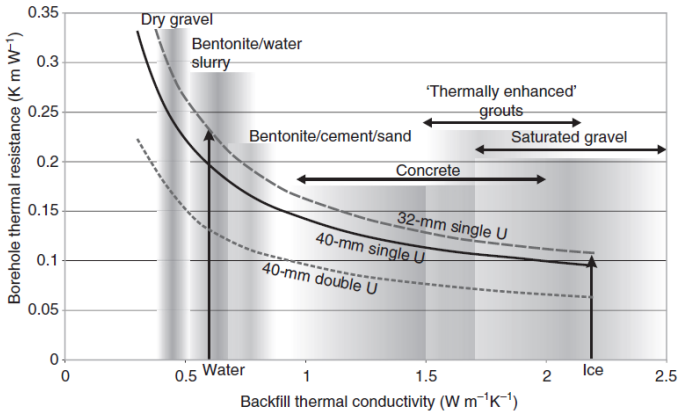

Figure 24: Typical range of thermal conductivities [24]

- Borehole diameter: smaller diameters ensure smaller resistance.
- Shank spacing: the flow channels should be kept at a large and possibly constant distance to minimise the short-circuiting. Therefore, based on Fig. 21, configuration C is the best possible, while configuration A denotes a poor installation of the U-tube. Spacers can be used, in order to maintain the constant distance.
- Heat carrier fluid flow rate: The aim is to ensure a fluid flow rate which creates a transient-turbulent regime inside the pipes. This state corresponds to a Reynolds Number between 2300-4000. After Re=4000, the flow is fully turbulent.

  In these flow conditions, the heat carrier fluid reaches a better contact with the pipe's wall, with higher heat transfer as a result. The goal is to have a fluid flow rate with a Reynolds Number higher than 2500 or, ideally, 3000. Over this value, the pressure loss becomes unacceptable [25].

Moving the focus from the single BH properties to an array, the mutual long-term interaction is of concern, since it can lead to excessive cooling of the ground and inefficiency of the system.

In order to limit BH interaction, one of the first measure to consider is the borehole spacing. A distance of minimum 15 m is recommended for example in the Ministry of the Environment guide [10]. Banks, instead, suggests a minimum distance of 10 m [24]. These values are obtained through considerations made upon small, single-family house systems, which only purpose is heating.

When the building requires also cooling, the borehole distance can be as low as 5 m, for reasons of regeneration of heat in the ground higher than in heating-only systems, thanks to the heat rejection during summer season.

Therefore, in heating only systems (or where heating is highly dominating) the required borehole spacing can be significant if one wants to obtain a low interference.

The extension of the construction area and the piping costs for a longer length can represent limiting factors.

To overcome these problems, an expedient is to incline the boreholes outwards, diverging from each other. This lets each borehole to have access to a wider volume of undisturbed bedrock. Figure 25a shows an example proposed by Eskilson of 8 boreholes in line on the surface, but inclined outwards at their basis.

Optimising a linear array can be achieved by drilling the boreholes inclined in alternate directions.

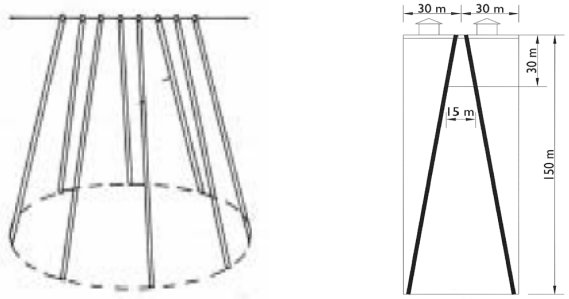

(a) Eight inclined boreholes [14] (b) Inclined boreholes [10]

Figure 25: Examples of inclined borehole configurations

However, a regular pattern is preferred, in order to simplify the piping and minimise its length.

A rectangular arrangement is more advantageous than one in line. In a line, pipe diameter needs to vary at each branch represented by a BH, since the flow volume increases towards the HP.

When, instead, BHs are in a rectangular shape, the solution is to have all small diameters but the header pipes to and from the HP.

Each BH can be considered as a single circuit connected in parallel to the other circuits, possibly through a manifold. A connection in series is normally avoided, for reasons of poorer heat collection and safety. A cold heat carrier fluid is circulated through the first borehole, collecting some heat; when it flows through the second ground heat exchanger, its temperature has already risen, reducing the available temperature difference between ground and fluid and the amount of heat that can be collected. Moreover, if there is the need of shutting off one BH, e.g. for a leak, every other borehole connected to the series will be closed.

Therefore, the normal practice is to arrange the boreholes to be connected in parallel with the other boreholes through a manifold. With a parallel configuration, the scope of having almost equal fluid flow rates in each borehole is more easily achieved. Each circuit is equipped with control valves, which are used to balance the fluid flow and shut off the circuit(s) if necessary. Manifolds allow to concentrate in one point the valves of several circuits (one manifold can accommodate up to 9-10 circuits), facilitating the control and maintenance.

One possible arrangement for BH and manifolds is shown in Fig. 26. The

manifolds are installed on the main lines, collecting the flows from different boreholes. This allows to minimise the piping length, with savings in both big diameter pipes, which are more expensive, and in terms of antifreeze volume required.

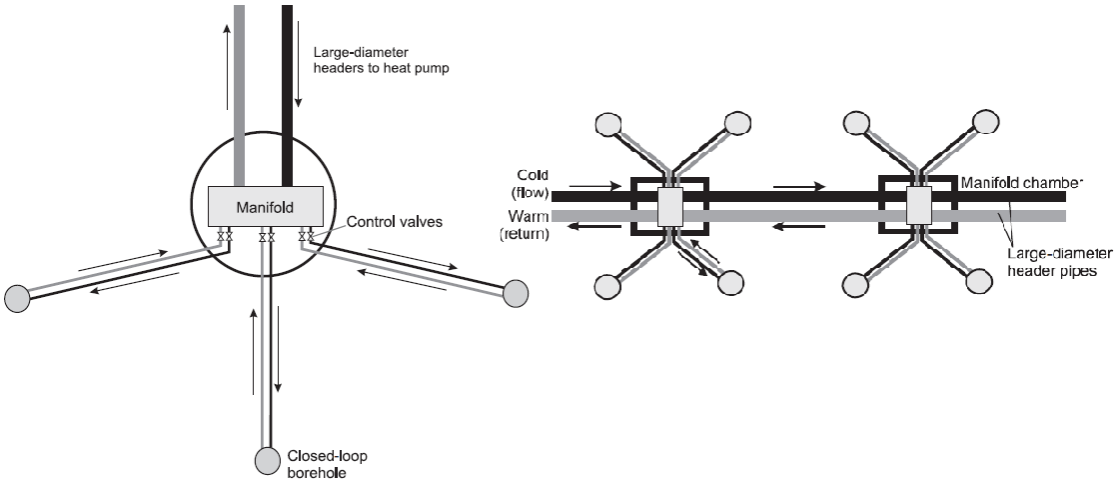

Figure 26: Example of manifold (left) and possible piping arrangement (right) [25]

4 Case study analysis

4.1 Geothermal system

4.1.1 Site characterisation

Finnoo project is under development and no accurate information are available on the soil properties, especially no TRT test is available for the area. Therefore, assumptions need to be made based on the available data.

Information on soil in Finland are provided by the Geologian Tutkimuskeskus (GTK), which developed maps freely accessible where soil types are characterised throughout the whole country [26]. This case study presents a soil which is composed of granite, rock with high thermal conductivity. The top layer (Fig.27) is mainly moraine and its depth is 11,65 m.

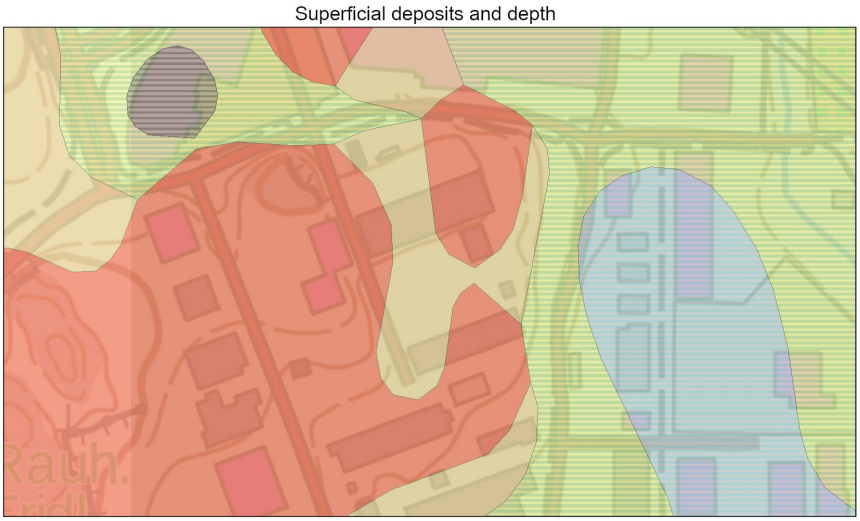

Figure 27: Superficial deposits and depth

GTK provides also maps which identify the geothermal energy potential in Finland. The maps' scale is 1: 1 000 000, with a cell size of 1 km^2. Therefore, these maps are not suitable for the actual sizing of geothermal systems, but anyway provide an idea of how potentially the area can be suitable for exploiting this resource.
The bedrock in Finnoo area is granite. The investigated depth for the maps is 300 m, which includes bedrock and the possibly overlaying quaternary deposits. At this depth, Finnoo bedrock has a renewable energy power of about 7862 W, and a stored geothermal energy of about 3.24 GWh.
The annual average temperature of soil in Finland can be considered as 2°C higher than the annual average for

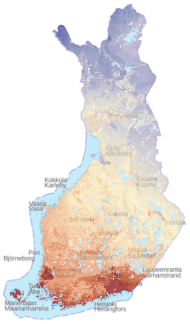

Figure 28: Geothermal energy potential

air. The temperatures vary according to the zone considered (e.g. southern region is warmer than northern regions) and there can be differences even inside the same area, since an area covered by forest is colder than one fully constructed.
After a certain depth, the temperature in the ground becomes independent from seasonal variations, so that it can be considered constant. In Finland, this happens after a depth of 10-15 m, as Figure 29 shows. The temperature gradient is in average 0.8-1.5°C/100 m and, in southern Finland, a temperature between 6.5 and 9°C can be considered for depths around 300 m.
In order to have an idea of soil characteristics in the Espoo area, two studies from GTK can be considered, one conducted in Nupurinkartano and one in Otaniemi. In Nupurinkartano [27], a TRT has been conducted in a 200 m deep borehole with single U-pipe. The bedrock is granite and its average thermal conductivity was calculated to be 3.50 W/mK. A geothermal gradient of about 1.1°C/100 m was registered for depths between 60 and 200 m. The borehole thermal resistance was assumed to be 0.08 mK/W.

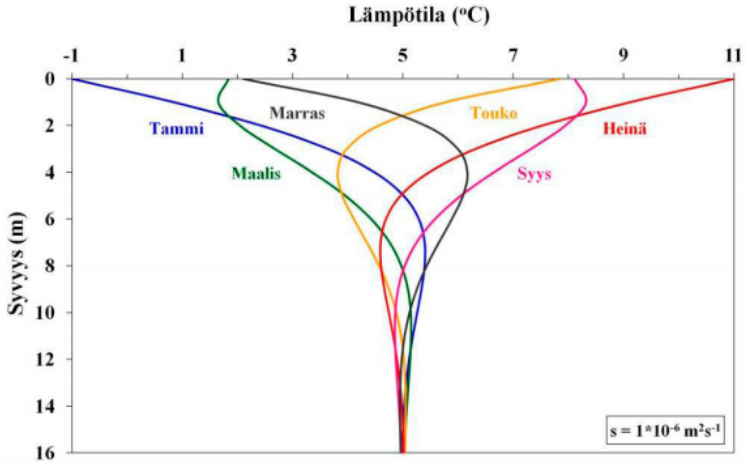

Figure 29: Theoretical heat-depth curves. Picture: Nina Leppäharju 2008 [28]

The second study [29] was conducted on the borehole thermal energy storage which serves the new building in the Otaniemi campus. TRT measurements were conducted in 300 m deep two wells. Bedrock is again granite, with measured conductivity between 3.2 and 3.4 W/mK. Borehole thermal resistances ranged between 0.095 and 0.1 mK/W, geothermal gradient of 1.19-1.3°C/100 m was measured. Temperatures at the well bottom were slightly over 10°C and overall average temperature along the borehole was as high as 8.8°C.

4.1.2 Case study borehole field

As previously mentioned, analysing the behaviour of several boreholes is a complex matter. Thus, the simulation approach has been used in this work and the software choice fell on Earth Energy Designer (EED).

EED is a software designed for HVAC engineers for reasonable and fast sizing of borehole heat exchangers. The software is equipped with databases containing

ground parameters for different locations, pipe sizes, materials and properties, as well as properties for several heat carrier fluids.

Moreover, it contains in a database a number of g-functions, among which one can chose the borehole configuration. Solutions are based on the calculation of the thermal response due to the given heat injection/extraction variations and the reciprocal thermal influence of boreholes, which is determined by the g-functions.

EED calculates the brine temperatures and heat extraction from the ground, based on heating/cooling loads. DHW can also be computed. These loads are easily inserted, as base loads (representing long-term heat extraction/rejection) and peak loads and their duration, which are inserted as monthly values. Peak loads are added at the end of the month during the calculation, to simulate the worst-case scenario. In the latest version of the software, it is possible to insert the loads as hourly profiles. Borehole thermal resistance and borehole length are also part of the output.

Beside the building loads, an important parameter is the Seasonal Performance Factor (SPF). EED simulates a ground source heat pump system: building loads represent only the input, while the ground loads are defined based on the SPF and coincide with the evaporator loads.

What is not possible to compute with EED is inclination, thus the simulated configurations are only for vertical boreholes.

Finnoo bedrock is granite. Database values are selected for thermal conductivity and volumetric heat capacity, which are respectively 3.4 W/mK and 2.4 MJ/m^3K. The soil surface temperature for Helsinki in the database is 5.6°C, while it is adjusted on 7°C for this simulation.

The boreholes have a diameter of 110 mm and, as it is common in the Nordic countries, they are assumed to be groundwater filled. Groundwater movement is of difficult computation and, even though it can be beneficial for heat transfer, to be on the safe side a thermal conductivity of 0.6 W/mK is used for the filling.

The ground heat exchanger is a 40 mm polyethylene single U-pipe, with thermal conductivity 0.42 W/mK and shank spacing 64 mm. With such pipe diameter, the flow rate considered is 0.7 l/s per borehole.

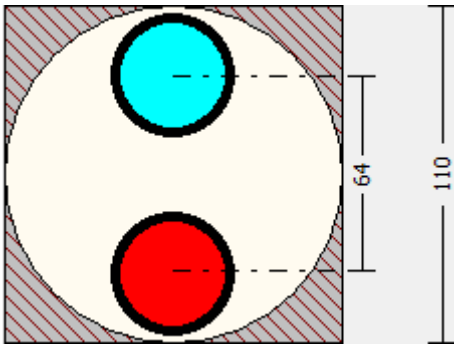

Figure 30: Borehole section from EED

Temperatures in the fluid are likely to go under 0°C, therefore an antifreeze solution must be used in the ground loop. Least harmful substances for groundwater

are ethanol and potassium formate solutions. Of these two, ethanol decomposes faster in contact with groundwater [10]. Therefore, a fluid 28% ethanol-water solution at 0°C is selected, with the following properties (from EED database):

Table 7: 28% ethanol-water solution at 0°C

Thermal conductivity	0.408	W/mK
Specific heat capacity	4216	J/kgK
Density	968	kg/m^3
Viscosity	0.0063	kg/ms
Freezing point	-18.5	$°C$

Since yearly load profiles are available for the area, they are used also for the simulation of the borehole field. Assuming that the energy demand will be somewhat similar in other years, the option to repeat the same profile over the whole simulation period is selected.

The choice is to dimension the heat pumps to provide the 60% of the peak space heating load. Thus, the profiles are adjusted so that the maximum heat output would be 1200 kW.

Space heating is provided to the buildings through underfloor heating, which requires a supply temperature of 35°C. On the other hand, domestic hot water requires at least 55°C. One can assume an SPF of 3.5 for space heating and 3 for domestic hot water.
For example, space heating load (Q_{SH}) to the ground would be:

$$\frac{Q_{SH}}{SPF} \cdot (SPF - 1) = evaporator \quad load \tag{4.1}$$

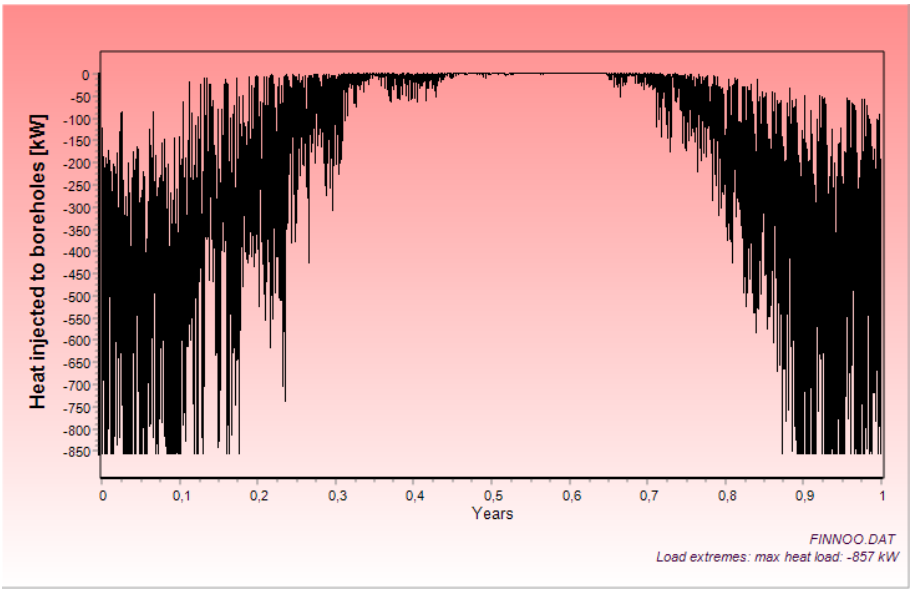

Figure 31: Evaporator (ground) load in Earth Energy Designer due to space heating

Borehole field geometry can be chosen among the g-functions available in the database. Fluid temperatures ever a selected period of time can be simulated and a second tool can be then run to adjust the borehole length if, for example, the one selected is overestimated. Instead of selecting and changing manually the g-functions, an optimisation tool is used. This allows for the software to run simulation against several g-function and automatically select the best configurations. Before running the tool, the available land area for borehole installation can be used, as well as ranges for borehole spacing and length.

A rectangular area of $230 \cdot 180m^2$ is selected from the Finnoo plot. Borehole spacing ranges between 5 and 25 m. The maximum depth is set to 300 m. Simulation time is 25 years, starting in September.

Four cases are simulated: a) SH only; b) SH and DHW; c) SH, DHW and SC (indirect) d) SH, DHW and SC (direct).

When considering space heating only, best configurations are found for a number of boreholes that ranges between 72 and 100, with borehole spacing from 25 to 20 m. Considering the two extreme cases, 72 boreholes require a length of 296 m, while with 100 the depth for each borehole goes down to 238 m. All are rectangular configurations. Minimum mean fluid temperature at the last year reaches -5°C and a maximum between 4.77 and 5.98°C, depending on the number of boreholes.

When adding domestic hot water load, inevitably the number of boreholes required increases and, because of the fixed available land area, their spacing reduces. Best configuration range from a minimum of 180 (depth 292 m, spacing 16 m) to 238 boreholes (depth 271 m, spacing 13 m). Minimum fluid temperature is again -5°C, but the maximum temperature is now slightly above 0°C. Figure 32 shows the slope of the temperatures over the entire simulation period, in the case with SH and DHW.

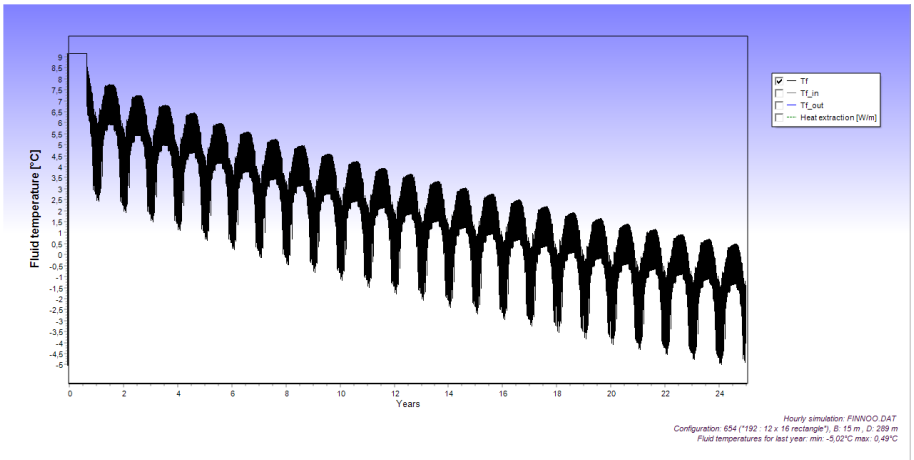

Figure 32: Mean fluid temperatures over 25 for space heating and domestic hot water

In case of indirect cooling, spacing is lower (13-14 m) than in the case with direct (free) cooling, as well as borehole depths. On the other hand, free cooling option shows a significant reduction in borehole number, which can be reduced down to

154 (spacing 17 m, depth 291 m). Both simulations show a minimum mean fluid temperature around -5°C, while the maximum temperature is between 13.5 and 14.5°C.

The best configurations for each simulated case are summarised in Table 8. The best configuration is chosen based on the number of boreholes and total length.

Table 8: Best borehole configurations for the four cases

Case	No bh	Grid	Spacing [m]	Depth [m]	Tot. length [m]
a	72	8 x 9 rectangle	25	296	21313
b	180	12 x 15 rectangle	16	292	52567
c	204	12 x 17 rectangle	14	249	50768
d	154	11 x 14 rectangle	17	291	44842

Option d) SH+DHW+SC (direct) is chosen for the area. For this configuration, the calculated borehole thermal resistance (fluid to ground) is 0.1167 (m·K)/W while the effective borehole thermal resistance is 0,1241 (m·K)/W.

For the coolest months, where all heat pump capacity is needed, the peak specific heat extraction rate is 30.8 W/m. In summer months, when only DHW is needed, specific heat extraction is as low as 13.8 W/m.

Minimum mean fluid temperature is found in February, equal to -5.02°C. Maximum fluid temperature of 13.5°C is registered in July. EED calculates also the Entering Water Temperature (EWT), which is the temperature of the fluid entering the heat pump, and the Leaving Water Temperature (LWT), which is the one that exits the heat pump system. Figure 33 shows the mean fluid temperature for the last year, while Figure 34 shows the heat extraction rate over the simulated period and EWT/LWT at the end of the 25th year.

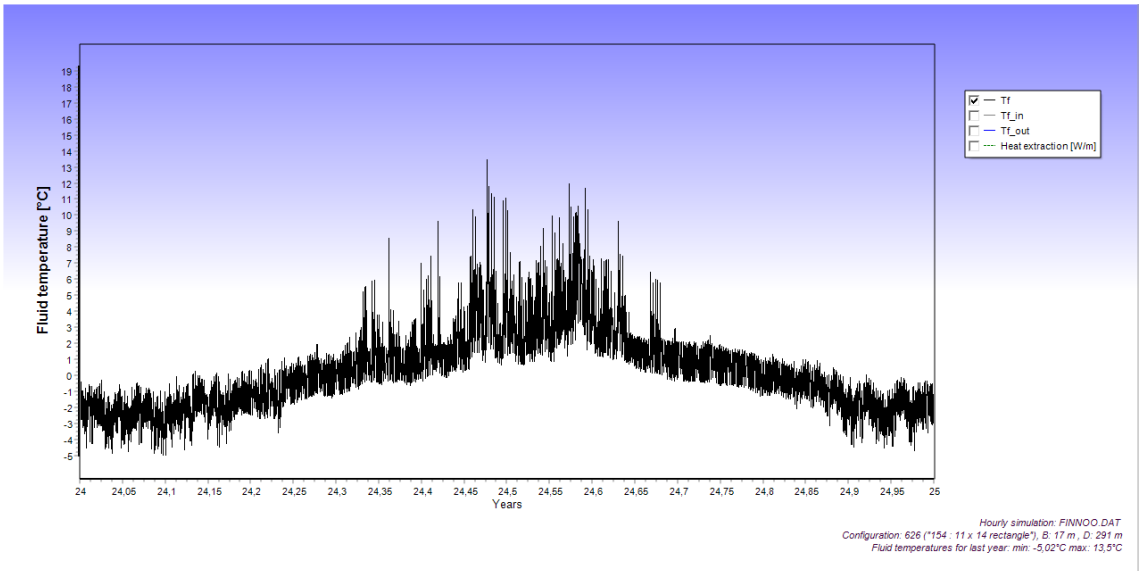

Figure 33: Case d) - Mean fluid temperatures in year 25

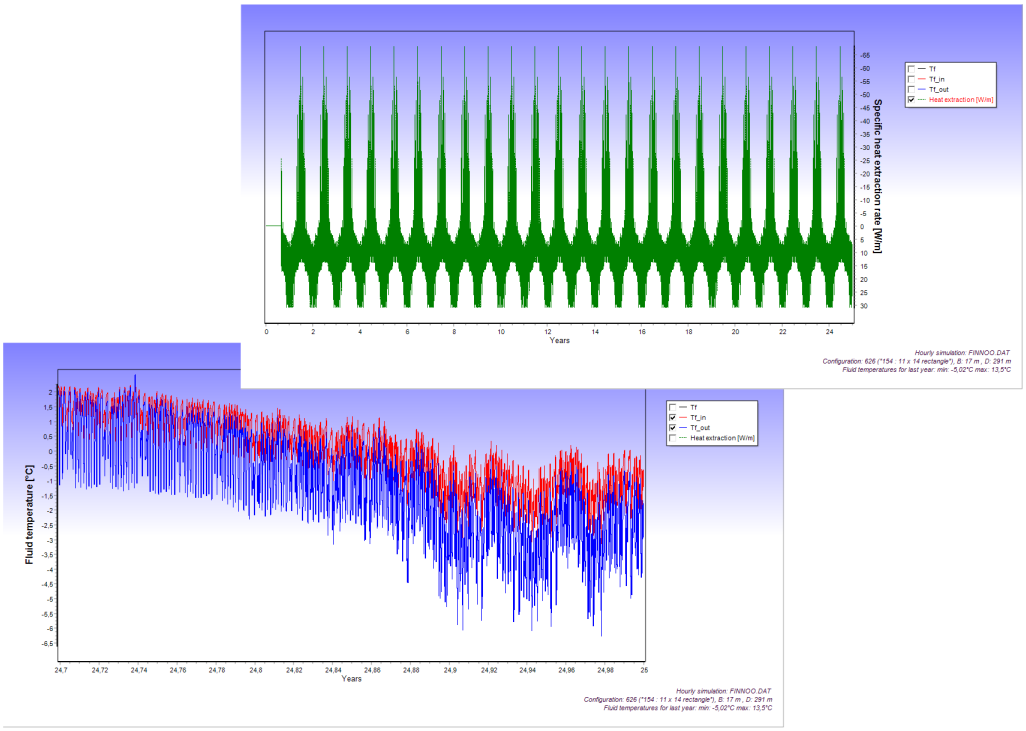

Figure 34: Heat extraction rate (top) and Entering (red) and Leaving (blue) Weater Temperatures (bottom)

4.2 Heating and cooling centralised plant

The area will be served from a centralised point, where all the energy systems will be located. The plant will contain the heat pumps, their buffer tanks and the heat exchangers, for the district heating backup, and the free cooling connection.

Each building is going to be connected to the local network via substations, for both district heating and cooling. The heated or cooled water is distributed to the ambient via the same floor piping. The water flow is controlled via the valve TV1, which closes in the summertime, making only cold water circulate in the underfloor piping (scheme adapted from Helen's guide "Kaukojäähdytyksen järjestelmäohje").

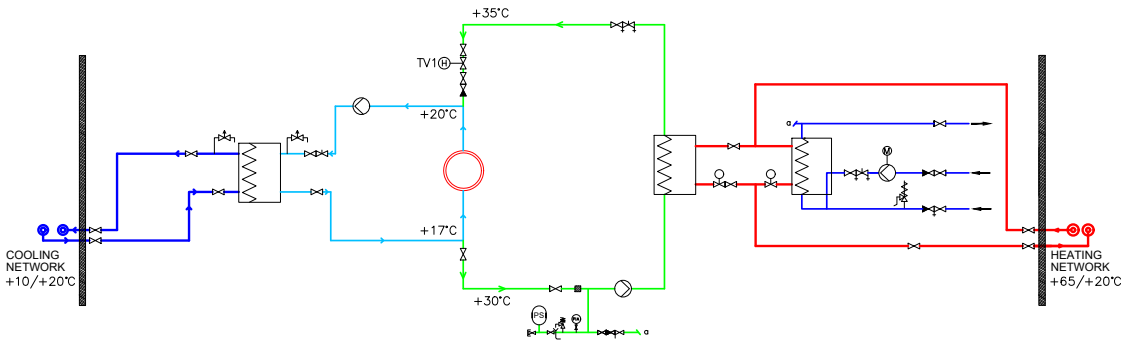

Figure 35: Example of floor heating/cooling with change-over

4.2.1 Heat pumps

The heat pump system is dimensioned to cover the 60% of the peak heating load for the area, which equals to cover up to 1200 kW. This way, most of the heating demand is covered only through heat pumps, and only a fraction by district heating.

Such load can be covered by three heat pumps of about 400 kW heating output each. For example, the Viessmann Vitocal 350-G Pro can be suitable for this case. It is a single-stage brine-to-water heat pump, with a screw compressor. Table 9 shows the heat pump performance for an output temperature of $45°C$, with COP calculated accordingly to EN 14511.

Even though this heat pump can reach output temperatures up to $65°C$, the performance factors of the heat pump tend to decrease, when high output temperatures are requested. Therefore, an output temperature of $45°C$ is selected.

Table 9: Heat pump performance data for an output temperature ($T_{w,out}$) of $45°C$, for different entering brine temperatures (T_{brine}). The columns contain, in order, rated heating output (H_{out}), rated cooling output (C_{out}), electricity consumption (E), coefficient of performance and energy efficiency ratio of the heat pump.

$\mathbf{T_{w,out} = 45°C}$					
$\mathbf{T_{brine}}$[°C]	$\mathbf{H_{out}}$[kW]	$\mathbf{C_{out}}$[kW]	**E** [kW]	**COP** [-]	**EER** [-]
-5	359	252	111	3.24	2.27
0	417	306	114	3.64	2.67
5	481	368	117	4.12	3.15
10	548	432	120	4.58	3.61
15	625	504	125	5.02	4.05
20	704	579	129	5.47	4.5
25	794	664	135	5.9	4.93
30	879	744	139	6.31	5.34

When installing multiple heat pumps, a parallel connection is preferred, since ensures a constant pressure drop for all the devices and avoids flow rate fluctuations during full load operation.

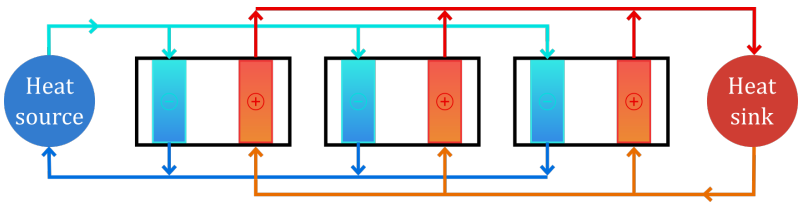

Figure 36: Parallel connection of heat pumps

In order for the compressor to operate without faults, the heat pump requires a minimum run-time, which maintains a minimum flow rate. This ensures also a minimum water volume to be present in the distribution lines. The minimum water

volume required is 3 l/kW of rated heating output, and needs to be available even when no heat is withdrawn from the system.

Buffer tanks are used to provide higher hydraulic stability, by ensuring this minimum water volume is always present in the system. For systems with small water volume, e.g. radiators, buffer cylinders are used to prevent excessive heat pump cycling. When operating with systems with high water content, e.g. floor heating, an overflow valve should be present to ensure the minimum flow rate.

A parallel connection of the buffer tanks has several advantages. Besides ensuring the minimum flow rate, buffer cylinders are also used to bridge power-OFF times, if any. Moreover, they provide hydraulic separation between heat pump and heating circuit, allowing the control of the minimum flow rate (q_{min}) in the heat pump independently from the secondary circuit, and they ensure longer running times.

In the case study, the water volume (V_{BT}) required for the buffer cylinders, for a heat pump output H_{out}, would be:

$$V_{BT} = q_{min} \cdot H_{out} = \tag{4.2}$$
$$= 3\frac{l}{kW} \cdot 417kW = 1251l$$

The total volume for three heat pumps is then $3.75m^3$. This can be fulfilled by using two buffer tanks with a capacity of 2000 l.

4.2.2 District heating connections

According to Helen's guidelines on DH, the local heat source, which can be solar heating or a geothermal or exhaust air heat pump, needs always to be connected in parallel to the district heating, to avoid that the return water is heated before it flows back to the district heating heat exchanger. Fig. 37 contains the connection example proposed in Helen's guide.

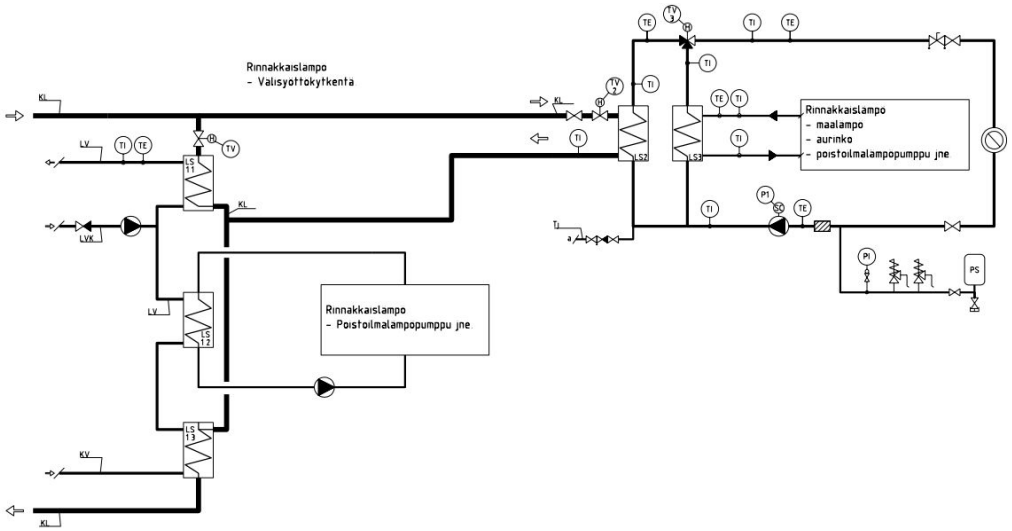

Figure 37: Example of connection between district heating and a parallel heat source

The space heating demand is covered primarily with the heat exchanger (LS3) which received the heat from the geothermal source. When and if the heat provided is not enough, the heat is transferred also through the DH heat exchanger (LS2). The heating network is equipped with a 3-way valve, through which the network can be adjusted. Due to large power variations, the DH heat exchanger is also equipped with two control valves.

Domestic hot water is produced through three heat exchangers, two are the DH heat exchangers (LS1.1 and LS1.3) and one is connected to the heat pumps (LS1.2). The water temperature is maintained at the desired value. The valve TV controls the flow of the DH, when the heat provided by the heat pumps is not sufficient to reach the set point. The LS1.3 acts as a pre-heater for the cold water.

This example is made for a single building, in which the domestic hot water and space heating are already separated. In the case study, only one heat exchanger is necessary. The district heating connection occurs inside the centralised plant, from where the heat is fed to a network, not the buildings already. Therefore, only a connection like the one for space heating in the example is considered.

The heat pumps are set to provide water at 45°C, while the district heating backup provides the heat to reach the 65°C needed for the supply.

4.2.3 Cooling

While the underfloor system is suitable to meet the indoor requirements with low temperature heating, the cooling works with high temperatures. This makes these systems easily coupled with boreholes and the use of free cooling.
Free cooling consists in circulating the heat carrier fluid between the buildings and the boreholes, without the use of a heat pump. This brings the advantage of utilizing electric energy only for circulation pumps, lowering running costs and carbon emissions.

4.2.4 Plant layout

Figure 38 and 39 show the proposed layout for the plant, respectively the heating mode and the cooling mode.

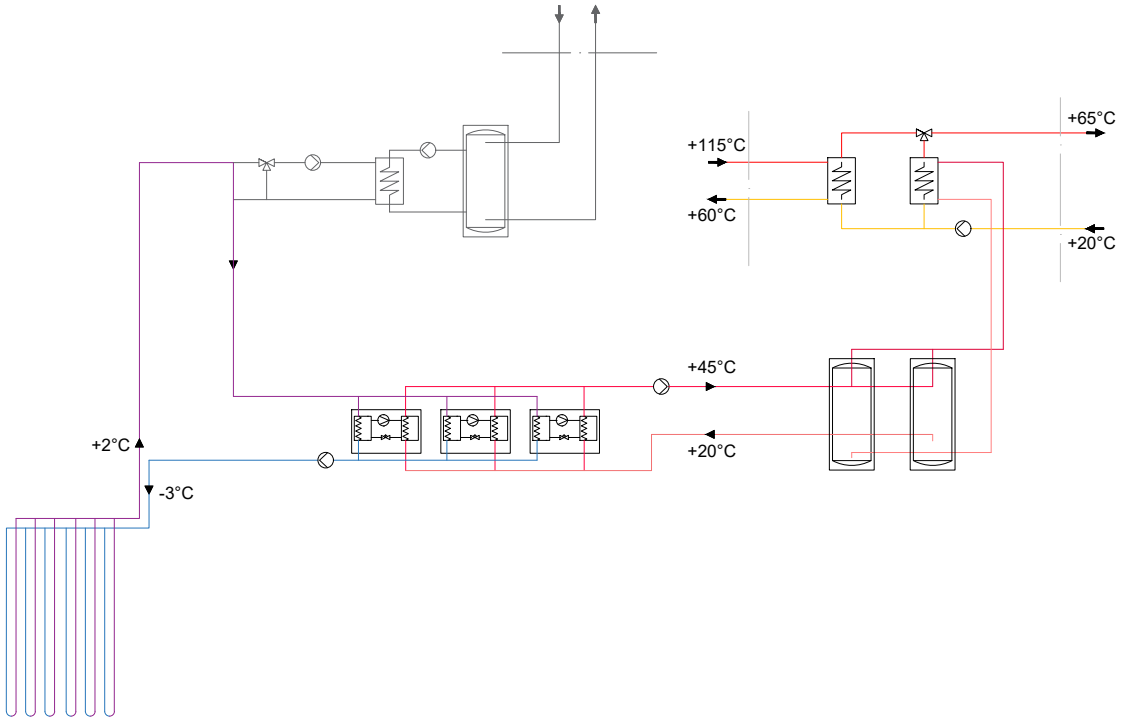

Figure 38: Plant layout in heating mode

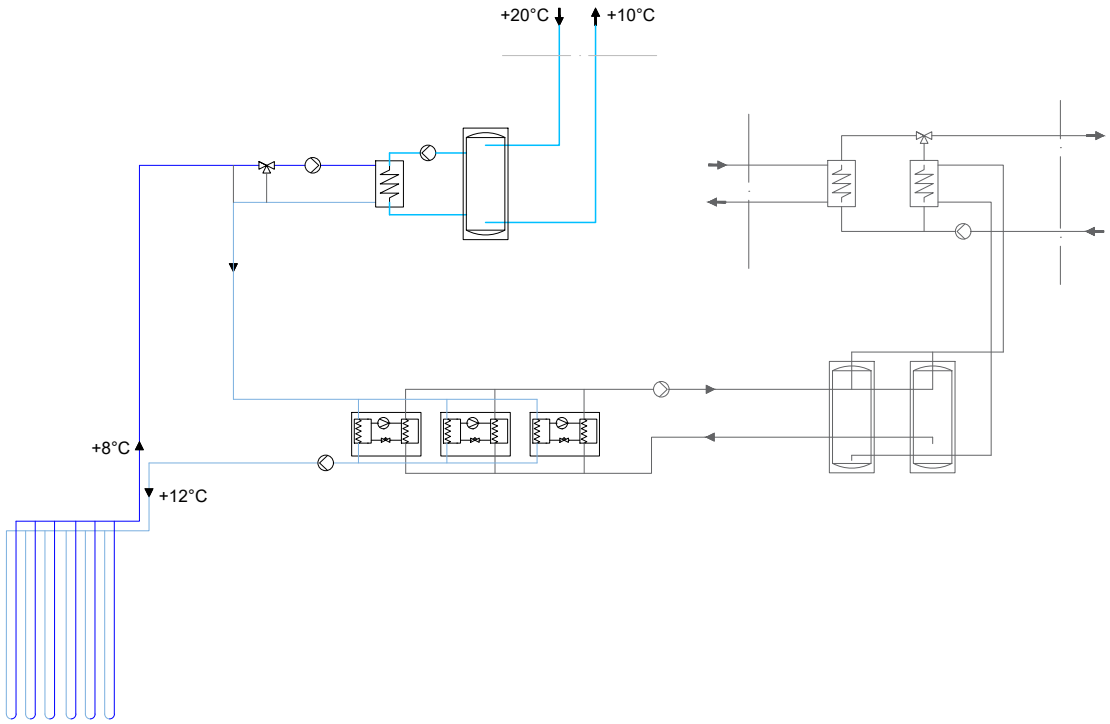

Figure 39: Plant layout in cooling mode

4.3 Distribution network - local low temperature energy network

The network is designed to supply heating and cooling to the buildings, therefore the goal is to size a four-pipe system: two for heating supply (SH and DHW) and two for cooling.
When sizing the heating network, the temperature constraint given by the domestic hot water needs to be considered. For health reasons, due to legionella risk, the water must be always kept at a temperature of at least 55°C (1047/2017).

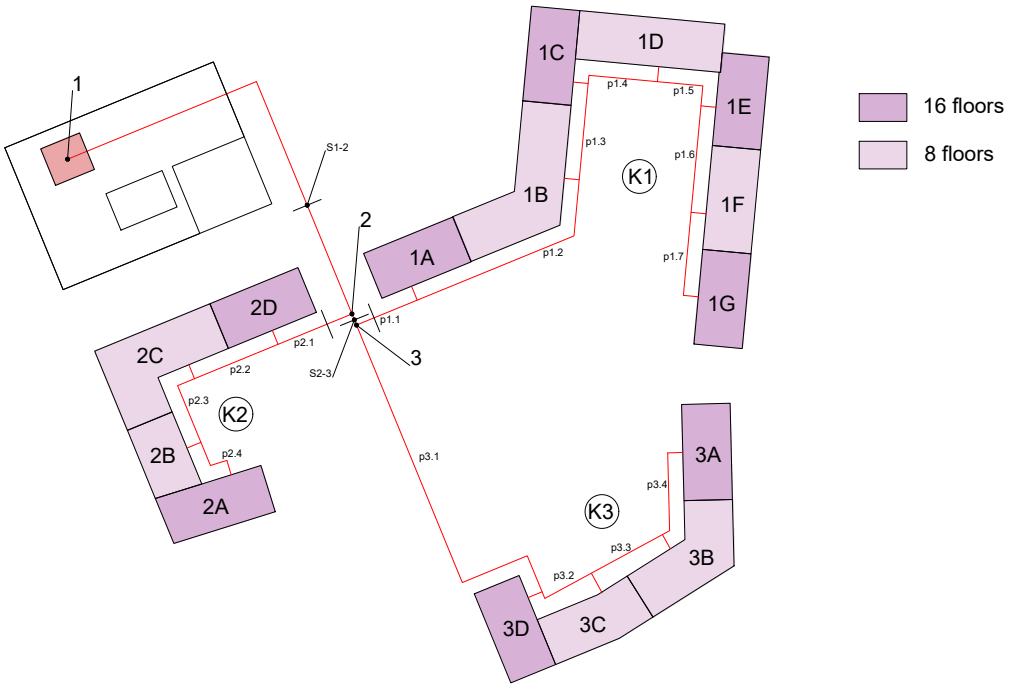

Figure 40: Network layout

Figure 36 shows the chosen network layout. A ring configuration, as proposed in [30], has an equal pipe length for every consumer, which leads to equalise the pressure differences between supply and return pipes and an easier control.
In this case, the construction process will take place in different phases, e.g. starting from the southern block (K3) and proceeding north afterwards. Therefore, a ring configuration would be too complicated to implement in this area.
District heating has supply temperatures which vary, according to the weather, between 65 and 115°C, and return temperatures between 40 and 60°C. Here instead, the aim is to have a low temperature heating network, which working temperatures are summarised in Table 9.

Table 10: Network temperatures

Network	Supply/Return temperatures
Heating	+65/20°C
Cooling	+10...12/20°C

4.3.1 Heating network

The low temperatures make possible the use in the heating network of plastic pipes. Plastic pipes are not affected by erosion like copper pipes, thus there is no limit to the flow rate velocity. Moreover, they allow significantly larger pressure drops.
First, the peak loads are defined, considering the design peak load simulated per m^2, which has been multiplied by the actual area of each building. The peak loads are summed up, starting from the last building, in order to obtain the load that each subsequent branch should carry.
Then, the corresponding flow rates (q) are calculated, according to Eq. 4.3:

$$q = \frac{Q_{peak,i}}{c_p \Delta T} \left[\frac{kg}{s}\right] \tag{4.3}$$

where $Q_{peak,i}$ is the peak load at each branch, c_p is the water specific heat capacity (4.2 kJ/kgK) and ΔT is the temperature difference between supply and return temperatures.
Pipes are sized according to the Uponor handbook on PEX-pipes [31]. The sizing criteria is based on the recommended pressure drop limits per unit length $\Delta P/L = 0.05 - 0.4 \quad kPa/m$.
Due to the flow rates, twin pipes result in having too small diameters, thus the choice fell on single pipes.
Table 11 summarises the results for the heating network. The pipes are considered buried at a distance of 5 m from the buildings. Building connections are DN50 pipes, and DN40 for buildings 2B and 2C.
The length of the network is 711.3 m and 75 m for building connections, for a total of 786.3 m.

4.3.2 Cooling network

Cooling network sizing would follow the same criteria and method used for the heating network. Here, the temperature difference is significantly lower than the one for heating, leading to higher flow rates. Since only the heating network is modelled and tested, the cooling network has not been taken into account.

Table 11: Heating network sizing. In order: q_m is the water mass flow rate calculated from the peak load, d_u/d_S are the external/internal pipe diameters, ΔP/L is the pipe pressure loss per unit length, v is the water velocity inside the pipe, HL is the pipe heat loss per unit length and L is the pipe length

	Pipe	**Peak load [kW]**	**q_m [kg/s]**	**d_u/d_s [mm]**	**ΔP/L [kPa/m]**	**v [m/s]**	**HL [W/m]**	**L [m]**
K1	p1.1	1406.8	7.5	110/90	0.12	1.2	26	21.82
	p1.2	1175.1	6.2	110/90	0.22	1.5	26	75.05
	p1.3	946.3	5.0	90/73.5	0.15	1.2	20	32.15
	p1.4	714.7	3.8	75/61.0	0.2	1.25	17	25.59
	p1.5	561.8	3.0	75/61.1	0.14	1	17	21.84
	p1.6	330.1	1.8	63/51.3	0.14	0.9	16	35.55
	p1.7	231.6	1.2	50/40.8	0.21	1	13	27.69
K2	p2.1	738.3	3.9	75/61.0	0.2	1.3	17.0	14.06
	p2.2	506.7	2.7	75/61.2	0.1	0.9	17.0	26.42
	p2.3	389.1	2.1	63/51.3	0.2	1.1	16.0	30
	p2.4	271.6	1.4	50/40.8	0.3	1.2	13.0	26.54
K3	p3.1	716.3	3.8	75/61.0	0.2	1.3	17.0	128.78
	p3.2	484.7	2.6	75/61.2	0.1	0.9	17.0	20.02
	p3.3	358.1	1.9	63/51.3	0.1	0.9	16.0	26.89
	p3.4	231.6	1.2	50/40.8	0.2	1.0	13.0	28.55
	S2-3	2123.1	11.3	110/90	0.3	1.8	26.0	3.99
	S1-2	2861.4	15.2	110/90	0.4	2.4	26.0	151.4
	Office	650.2	3.4	75/61.2	0.2	1.2	17.0	15

4.3.3 IDA ICE network model

The network model is developed in IDA ICE, based on the components developed by Nageler [32]. The aim is to test if a local low temperature (65°C supply) is able to satisfy the area requirements. First, a network that considers a typical district heating supplier is modelled, with constant supply temperature of 65°C. Secondly, the network supply is realised by ground source heat pumps (GSHPs) with district heating as additional heat source for peak loads.

Network components

The network is built upon three main components: supplier model, pipe models and a substation (customer) model.
The supplier model defines the supply temperature and pressure available at the network inlet.
The pipe models used are finite difference element objects and they are divided in segments of about 2 m. A pipe has only one inlet and one outlet, therefore the multi-branch model is used, in order to allow the connection of multiple pipes, e.g. where the customer connection to the main line occurs.
The substation model creates the link between buildings and network models, simulating the heat exchanger that separates primary and secondary side in a real district heating network.

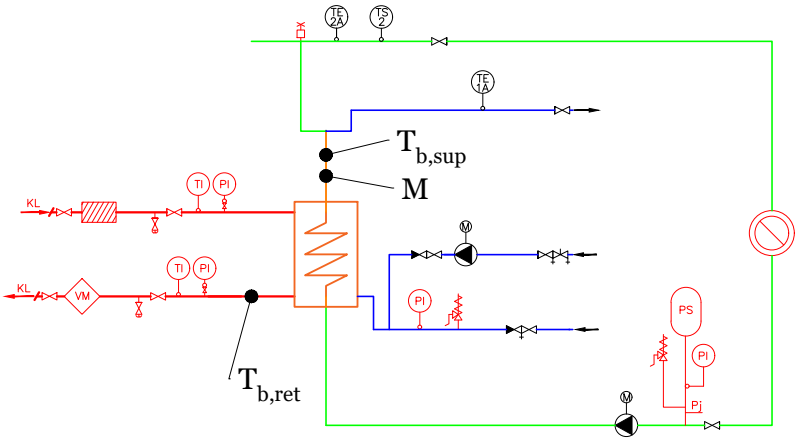

Figure 41: Simplified substation scheme and main variables

It is a simplified model of a district heating substation, since it includes only one heat exchanger.
The building is represented in this environment by its load profiles, that account for both space and domestic hot water heating loads due to the simplifications at the substation level. These profiles are first processed by a macro, which calculates the necessary mass flow (M) and return temperature ($T_{b,ret}$) for each building, based on the desired temperature difference. Then, these results are used as input values for the substation.

Such model computes the outlet temperature after the heat exchanger ($T_{b,sup}$), considering a certain efficiency of the heat exchanger and the return temperature previously obtained from the load profiles. As output, one gets a temperature that is the overall temperature fed to the building for both space heating and domestic hot water.
On the primary side of the heat exchanger, a throttle valve controls the mass flow so that it equals the mass flow requested from the consumer. If the differential pressure on the primary side is no longer sufficient, the mass flow on the primary side drops.
Figure 40 shows how the geometry of the network has been implemented in IDA ICE. The pipes are sized according to the data in table 11.

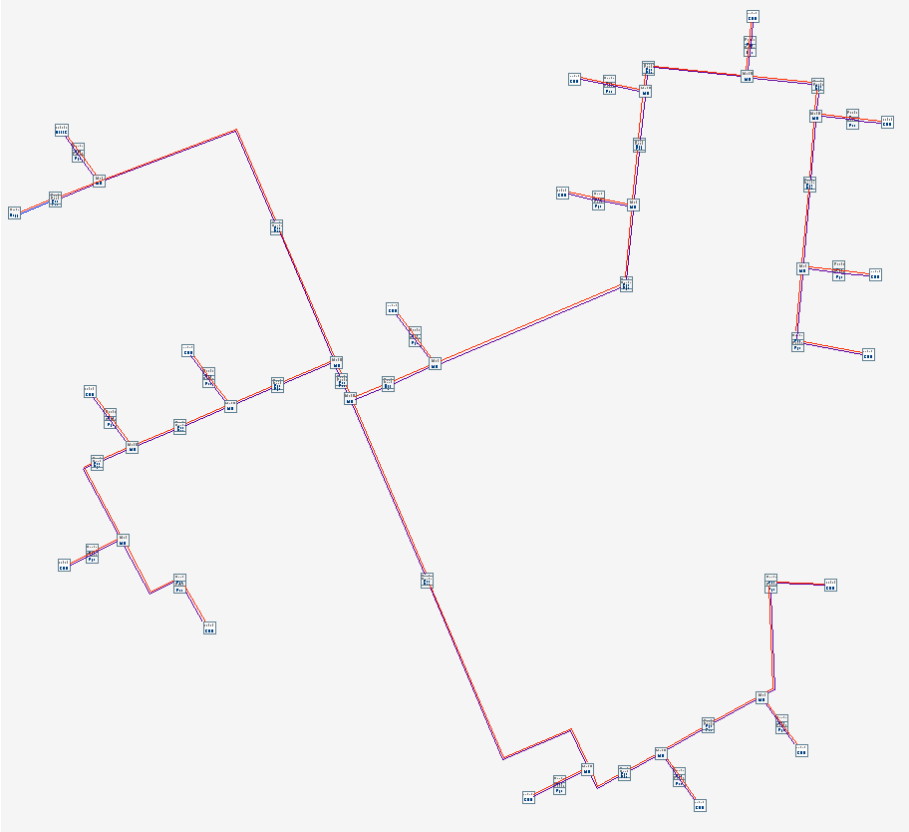

Figure 42: Heating network in IDA ICE

The network computes the temperatures reaching each client, mass flows and heat losses. Considering that the domestic hot water must be always above 55°C because of legionella risk, the supply temperature to the building must be always above it. A check has been made on the temperatures that reach the furthest customers (1G, 2A, 3A) in the case of low temperature network.
The district heating network proves to be able to deliver the required temperatures if the initial node supplies a temperature of only 65°C. The minimum supply temperature occurs at the customer 1G and is slightly below 61°C. The minimum occurs during May, meaning that only domestic hot water is needed, so the temperature is high enough to fulfil the heating requirement.

Network model with heat pumps

In order to insert the complete plant, a macro object was created.

The boreholes are modelled according to the EED results. The same properties for ground, pipes and heat carrier fluid are used, as well as for geometrical properties. The borehole model allows to analyse only a portion of the total grid through a mirroring function. The results for the whole field are computed using superposition. The boreholes are mirrored around Cartesian symmetry axes, assuming that the holes are equally spaced around the axes and that the coordinates are centred around the origin.

In this case, of the 11x14 grid, only 42 boreholes are computed, as shown in Figure 43. Out of these, 35 boreholes (red) are mirrored symmetrically into the other three quadrants, while the remaining 7 (pink) are mirrored only over the y-axis.

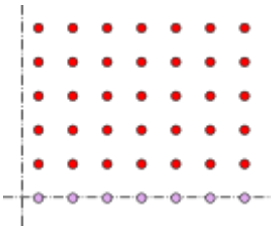

Figure 43: Simulated symmetric boreholes

The borehole model is then linked to three heat pumps, which are connected in parallel. The heat pumps control consist of a PI controller, which sets the requested temperature to 45°C. The power and COP are inserted accordingly to the chosen heat pump data.

After the heat pumps, a heat exchanger simulates the district heating backup, with a flow temperature on the primary side of 115°C.

From this point, the plant is connected to the supplier model, previously described, through which the network is fed. Now, the supply temperature is not constant, but varies based on demand and heat pump operation.

Only the heating network has been modelled. However, the borehole field was sized to provide free cooling, meaning that some heat is rejected to the ground. If cooling is not considered, the temperature in the ground will drop significantly.

The cooling effect is then taken into account through a load profile, which simulates the heat rejection to the ground. In order to maintain realistic temperatures, only 70% of the full load is considered. The values are positive, in order to indicate heat rejection to the ground.

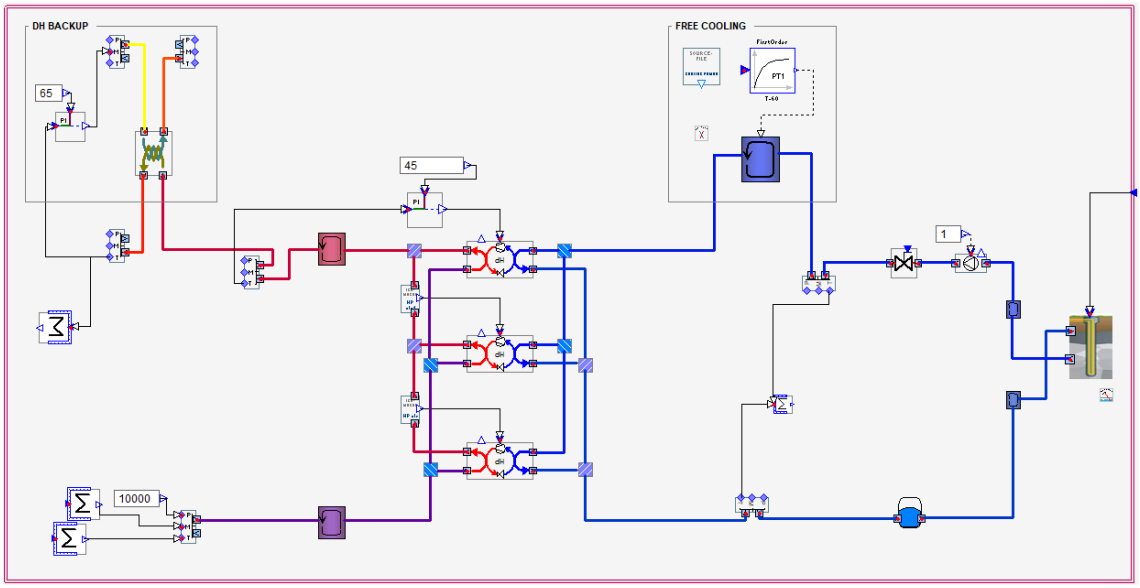

Figure 44: Plant implemented in IDA ICE

The network operation is simulated for 25 years, starting in September. Like in EED, the profiles are repeated similarly for each year.

5 Economics and sustainability

5.1 Life Cycle Cost

Life Cycle Cost (LCC) analysis is used to estimate if an investment is profitable. The calculation includes investment and operational costs. The general expression is:

$$LCC = \sum_{k=0}^{n} \frac{I_k}{(1+i)^n} + \sum_{k=1}^{n} \frac{C_k}{(1+i)^n} - \sum_{k=1}^{n} \frac{P_k}{(1+i)^n} - \frac{R}{(1+i)^n} \tag{5.1}$$

where

I_k: investment cost, €

C_k: annual costs (at the end of the k-th year, including energy, service and maintenance costs), €/a

P_k: annual profits (at the end of the k-th year), €/a

R: residual value at the end of the analysis period (n-th year), €

$d = \frac{1}{(1+i)^k}$: discount factor, where i is the nominal interest rate, %

Within the different methods for evaluating the profitability of an investment, one of the most common is the Net Present Value (NPV). The method calculates the present values of future cash flows over the lifetime of a system, taking into account interest rates and inflation. If the NPV results positive, the investment is profitable.

$$NPV = \sum_{k=1}^{n} \frac{C_k}{(1+i)^n} - I_0 \tag{5.2}$$

Another index of profitability is the payback period n_d, that indicates the time span by which the incomes generated by the investment will equal the initial capital, I_0. The discounted payback period, which includes the influence of interests, is calculated as:

$$n_d = \frac{ln\left(1 - \frac{I_0}{C} i\right)}{ln\left(\frac{1}{1+i}\right)} \tag{5.3}$$

The investment costs are assumed to be paid all at the beginning. In the investment are considered the heat pumps and the buffer tanks, the borehole costs and the distribution piping's costs. An annual maintenance cost, equal to 1% of the investment cost, is used for the GSHP system [33].

The cost for the heat pumps is estimated based on the prices retrieved from a seller's website [34], from where the average specific price per kW is calculated. The buffer tank cost is calculated according to the IEA proposed cost function [35] for tank volumes between $0.5m^3$ and $500m^3$, resulting in $925€/m^3$. A total of three buffer tanks are considered, two for heating and one for cooling.

Borehole drilling cost for one or two wells is around 30-35€/m. The price rises to 35-40€/m for bigger borehole fields. Moreover, the price is different, if the drilling

occurs before reaching or inside the bedrock, being the first one in the range of 40-60€/m [36]. Therefore, they are considered as two separate entries, with a soil cover depth of 11.65 m. The prices include the piping, insulation and connection of the boreholes.

The price of the heating distribution pipes depends on their diameter. The prices are defined according to Uponor Ecoflex Thermo Single price list [37]. The table displays only the average price, while the total account for the different diameters. Assuming the cooling network composed of similar PEX-pipes and having the same length of the heating network, the same total price is used.

Pumps for circulating the heat carrier fluid in the borehole loop and for the local heating network are needed. Their price is considered as total of 10000€, as suggested in [38].

Table 12: Investment cost components

Components	**Unit cost**		**Tot. quantity**	
HP	280	€/kW	1251	kW
Buffer tanks	925	€/m^3	6	m^3
Pumps	10000	€	1	
BH drilling (soil)	58	€/m	1790	m
BH drilling (bedrock)	38	€/m	43020	m
Local network heating pipes	70.4 (avg)	€/m	1573	m
Local network cooling pipes	70.4 (avg)	€/m	1573	m

A real interest rate (r) of 3% is chosen accordingly to the Commission Delegated Regulation No. 244/2012 [39]. The real interest rate takes into account the effects of inflation. The general inflation f can be calculated from the Consumer Price Index [40], according to Eq. 5.4.

$$f = \left(\frac{IND_2}{IND_1}\right)^{\frac{1}{t}} - 1 \tag{5.4}$$

where IND_i is the price index in a certain year and t is the time difference between the two points in years.

Energy prices vary differently as compared to general inflation. Therefore, it is necessary to define their specific inflation or escalation e, following the same principle of the general inflation. Escalation for electricity is based on the Elspot historical data retrieved from Nord Pool website [41]. Similarly, escalation for district heating is determined based on statistical data provided by Energiateollisuus [42]. The data refer to the last 10 years and they include taxes. Calculated escalation for electricity is -5.8%, showing a negative trend in the prices. Therefore, a conservative 1% [43] is used. On the other hand, district heating price shows an escalation of 4%.

The real interest rate for energy, which includes the escalation effect is calculated according to Eq. 5.5. The results are simply replaced to i when calculating the discount factors (d).

$$r = \frac{i - e}{1 + e} \tag{5.5}$$

With a calculated inflation of 1.3%, the real interest rates for electricity and district heating are, respectively, $r_{e,el} = 3.3\%$ and $r_{e,DH} = 0.3\%$.

Energy costs are chosen as the average yearly price for 2019. The operational cost of energy (C_e) is calculated as:

$$C_e = \sum_{k=1}^{n} \frac{c \cdot Q_k}{(1 + r_e)^n} \tag{5.6}$$

where

c is the energy price [€/MWh]

Q_k is the yearly energy consumption [MWh]

$d = \frac{1}{(1+r_e)^n}$ is the discount factor

Yearly maintenance cost (M_k) is calculated according to:

$$M_k = \frac{0.01 \cdot I_0}{25y} \tag{5.7}$$

Thus, the total maintenance cost (M) is calculated as:

$$M = \sum_{k=1}^{n} \frac{M_k}{(1 + r)^n} \tag{5.8}$$

For comparison, a system where all the heat demand is provided through district heating is used. Its investment cost is calculated, for one building, as 15 500 €, which includes basic charge, water flow charge and the piping connection. The price is retrieved from other projects of the company with similar peak power. The maintenance cost used is 0.5% of the total investment cost.

5.2 CO_2 emissions

The use of heat pumps, thus producing energy locally, reduces the CO_2 emissions, since the consumption of district heating is lower.

The calculation of the CO_2 emissions consists in multiplying the energy consumption by the emission factor, differentiated by energy carrier. When evaluating the geothermal system, the electricity consumption of the heat pumps and the district heating backup are considered.

$$CO_2 emissions = \varepsilon \cdot Q_e \tag{5.9}$$

where ε is the emission factor (see Table 13) $[kgCO_2/MWh]$ and Q_e is the energy consumption [MWh].
The emission factors for energy production are retrieved from Motiva [44], and they are representative of the average emissions of the last 5 years.

Table 13: CO_2 emissions by energy carrier

	$\mathbf{kgCO_2/MWh}$
Electricity	141
District heating	154

6 Results and discussion

6.1 Simulation results

In the following, simulation results of the borehole field together with the local network, are presented.

The overall required heating energy results in an average of 15540 MWh/a. The chosen setting of the plant, with a heat pump output temperature set to 45°C, is able to produce 70% of the heating energy by heat pumps and only 30% is required from the backup heating (Fig. 45).

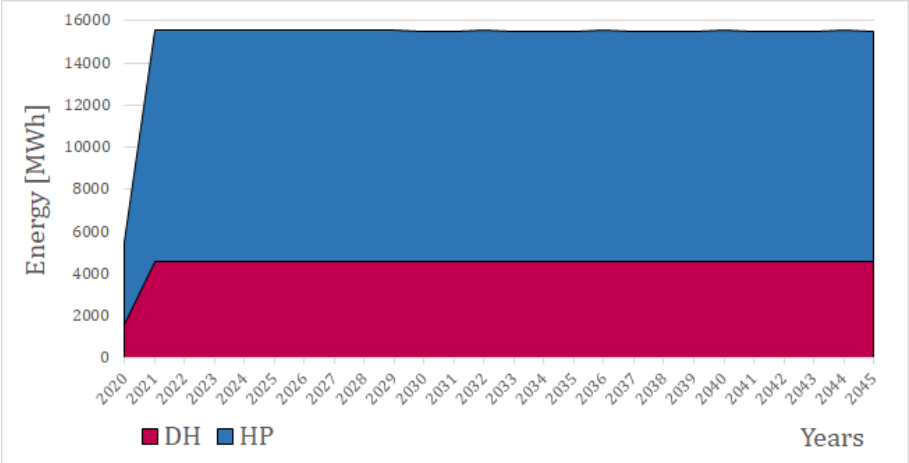

Figure 45: Energy share between heat pumps (HP) and district heating (DH)

Even though there is a mismatch between EED and IDA solution for entering and leaving fluid temperature from the boreholes, the mean fluid temperatures are close, over the whole simulation period (Fig. 46).

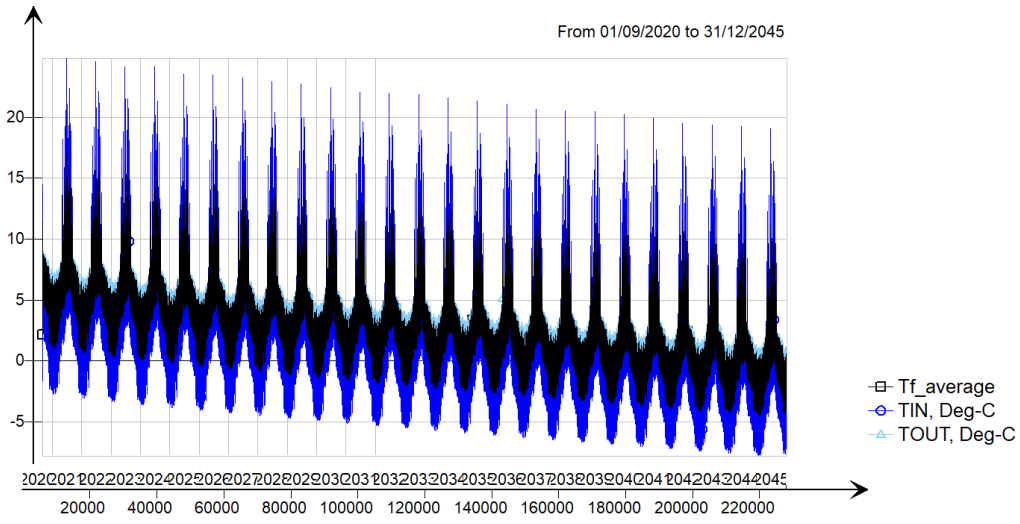

Figure 46: Borehole temperatures simulated in IDA ICE

The heat pump performance is evaluated from COP and SPF values. The three heat pumps have been simulated with the same settings, therefore it is assumed they have similar performance. COP ranges from a maximum of 4.3 in the first year to a minimum of 3 in the last year. Overall, the average COP is equal to 3.4.

The average SPF per year is shown in figure 47. The reason for the slope is that, over the 25 years, it occurs a slight decrease in the heat pumps' output and a slight increase in their electricity consumption.

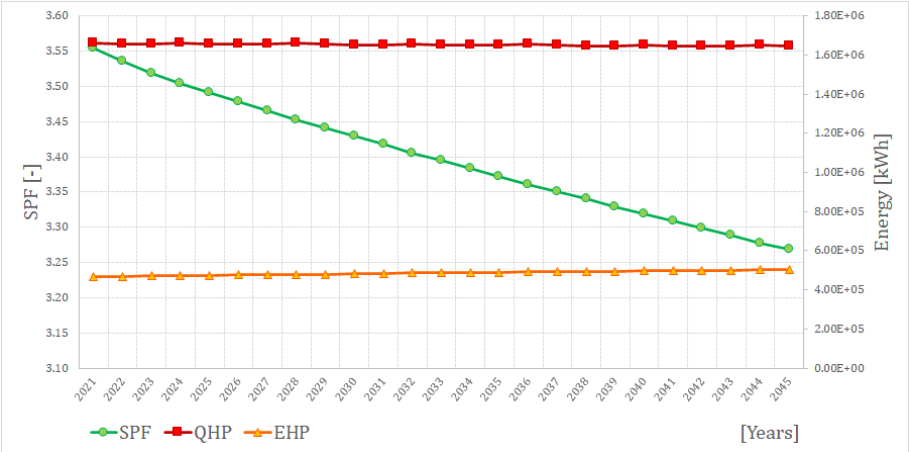

Figure 47: Heating output (QHP), electricity consumption (EHP) and seasonal performance factor (SPF) for one heat pump

The network is able to provide hot water to all the buildings, with temperatures ranging between 65 and 61 degrees, depending on the season and how far the customer is from the supply point. Figure 48 shows the distribution of the supply temperatures reaching each customer over the whole simulation period.

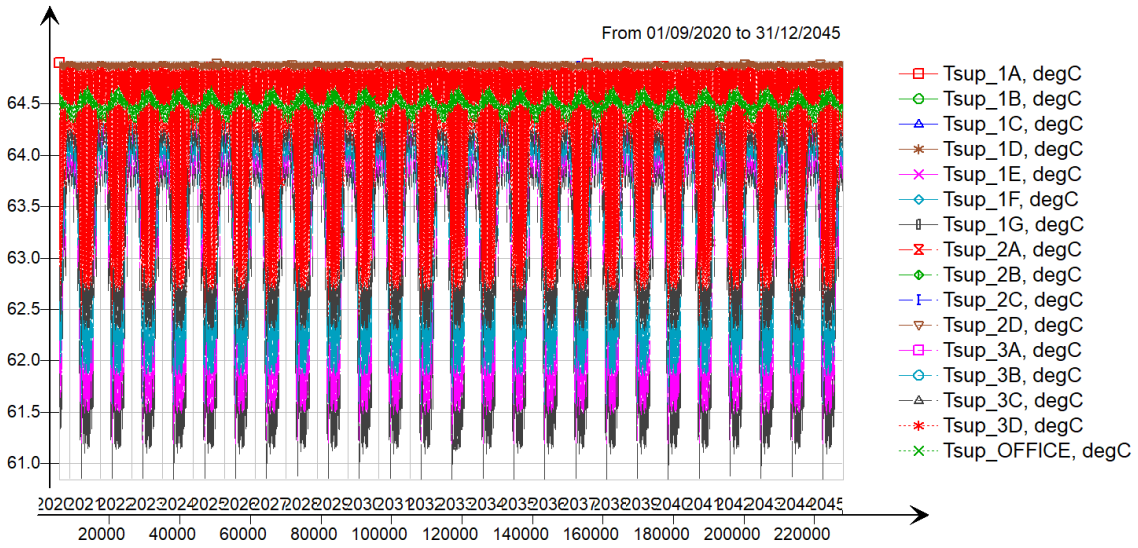

Figure 48: Temperature ranges (y-axis) over 25 years (x-axis). Tsup are the supply temperature for the different customers

6.2 Life Cycle Cost results

Figure 49 shows the components of the investment cost for the GSHP system. The most contributing component is the borehole drilling and, together with the heat pumps investment, these two entries cover up the 86.7% of the total investment cost. The other components have a small impact, especially buffer tanks and pumps.

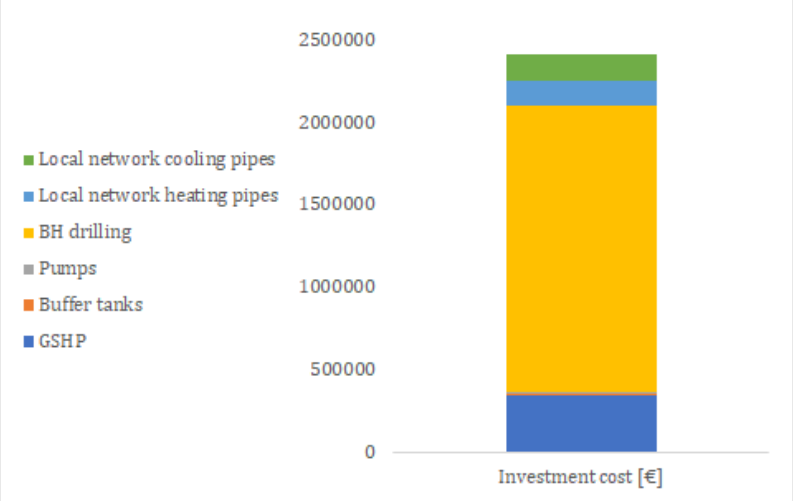

Figure 49: Investment cost for ground source heat pump (GSHP) system

Table 14 reports the detailed values for the calculation of the Net Present Value, for both GSHP and DH only systems.

Table 14: Detailed Net Present Value (NPV)

Cost	**GSHP**		**Cost**	**DH**	
Investment costs					
GSHP	350280	€	Connection cost	248000	€
Buffer tanks	5547	€	Local network heating pipes	152092	€
Pumps	10000	€			
BH drilling (soil)	103826	€			
BH drilling (bedrock)	1634756	€			
Local network heating pipes	152092	€			
Local network cooling pipes	152092	€			
Operation costs					
Imported electricity	1098061	€	Imported DH	29117323	€
Imported DH	8580668	€	Maintenance	1473	€
Maintenance	17740	€			
NPV	7 287 874	€	**NPV**	28 718 704	€

The investment cost for the reference case is significantly lower than the one required for the GSHP system. On the other hand, the NPV shows the opposite trend, with a value of 257.5€/m^2 for the DH and 65.4€/m^2 for the GSHP. The higher the NPV, the more profitable would be the investment.

However, when considering the purchased energy, the GSHP system seems more convenient than the reference case. Looking at the operational costs for energy, the overall price, referred to 1 m^2 of net-heated area, is 87 €/m^2, while for the DH only system is 261 €/m^2. The energy costs distribution over time per m^2 is shown in figure 50.

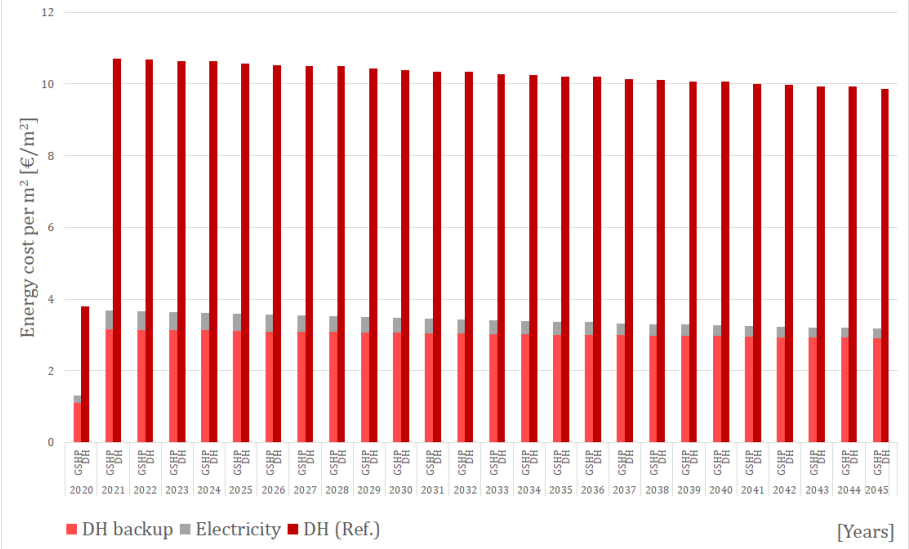

Figure 50: Yearly energy cost per m^2 over the system's life cycle

The calculated payback period for the GSHP system is 9.7 years. When this time is smaller than the life span of the system, it indicates that the investment would be profitable. This period is lower than the considered life span of the system, indicating that the investment seems profitable and would start generating savings in about 10 years.

6.3 CO_2 emissions results

The CO_2 emissions have been calculated according to table emission values. Electricity total emissions over the calculation period are 5216 tCO_2, while the district heating backup contributes for 17885 tCO_2. If all the heating comes from purchased district heating, the total amount of emission raises to 60688 tCO_2.

Figure 51 shows the emissions per year.

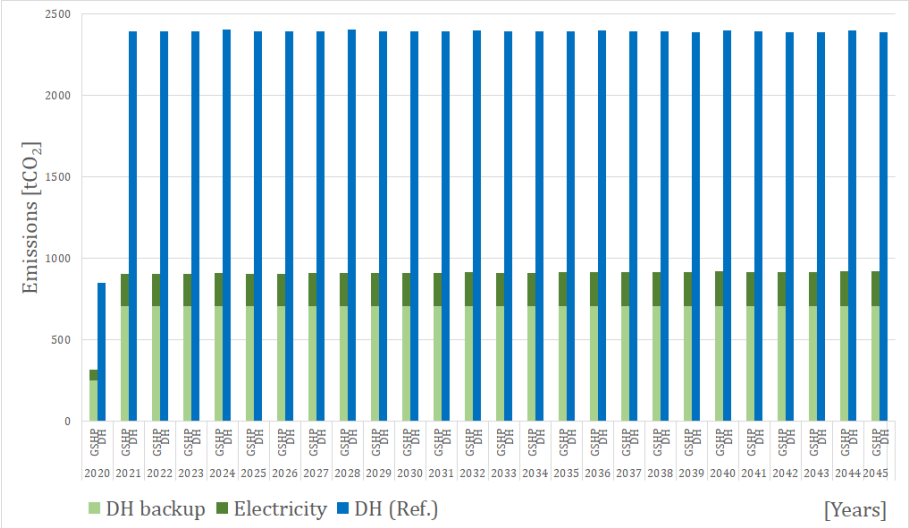

Figure 51: CO_2 emissions for 25 years

6.4 Discussion

The aim of this research was to analyse alternative energy sources for supplying heating and cooling to a new neighbourhood. The main idea was to utilise geothermal energy as the primary source and centralise all the necessary appliances in one plant, which would be located inside the office building. The proposed solution found that three heat pumps, for a total output power of 1251 kW, are able to provide up to 70% of the total area heat demand. District heating provides for the remaining 30% of the energy. It represents the main source of heating in the Helsinki metropolitan area, thus it is promptly available and a stable heating source. The choice of this kind of backup was also based on the fact that the Suomenoja CHP plant is located close to the area under analysis and piping line is already existing on its perimeter.

The low temperature heating network seems to have potential application. Newly constructed buildings would easily allow a connection to such network, since floor heating (cooling) systems require lower (higher) temperatures than, for example, radiators. Thus, supply temperature requirement is only dictated by the DHW. The target supply temperature was 65°C. Its oscillations in the simulation results are due to the length of the line between the supply centre and the consumer, and to the demand profile. Simulations show that the supply temperatures remain always above 61°C. Even in the worst case, the furthest customer, temperatures are above 64°C for 80% of the year. The drop in temperature occurs during summertime, and can be ascribed to the lower heating demand, which is now represented only by DHW.

Even though the target supply temperature is 65°C, it has been chosen to set the heat pumps to provide a temperature of 45°C, for efficiency reasons. It is known that the larger the temperature difference between evaporator and condenser, the lower the COP. If heat pumps were to deliver a temperature of 55°C, the heating

coverage would raise up to 80%, but the COP would decrease over the years down to 2.3, compared to a 3.0 in the chosen case.
The use of heat pumps makes possible to cover a large share of the heat demand by renewable energy. This translates to a decrease in the imported energy and a consequent reduction in the CO_2 emissions. Compared to the reference case, the amount of purchased energy is 61% lower, and the difference in purchased district heating is up to 71%.

This trend is reflected in the operational energy costs, which show that savings of 66-68% can be achieved yearly. The 2 408 594 € investment cost for the GSHP system is significant, and the borehole drilling accounts for more than 70%. However, geothermal systems are becoming more and more common and their drilling price might decrease in the upcoming years, so a new evaluation when this project will be ready for construction might lead to a lower investment cost.

The positive NPV indicates that the investment is profitable. The discounted payback period indicates that the initial costs would be covered in 9.7 years and, being shorter than the assumed life span of the system, the investment can be again regarded as profitable.

Being the CO_2 emissions a function of the energy consumption, they follow the same trend. The reduction is calculated as 62% from the reference case. In the GSHP system, electricity accounts for the 23% while the backup is responsible for 77% of the emissions.

Must be noticed that the reference case is used mainly for comparison on energy prices and CO_2 emissions, and not for comparison of the investment cost and NPV, because of its rough estimation.

Cooling system was not considered in detail, since Finnish climate is highly heating dominated. On a yearly basis, cooling represented only 11% of the total energy demand. Nevertheless, when planning borehole fields, solutions for heat soil regeneration must be taken into account. In this case, the heat rejection due to cooling prevents the soil temperatures to drop significantly and maintains the system operational up to 25 years.

Limits and uncertainties of the analysis

The sizing of the local hybrid energy system is based primarily on heating and cooling load profiles, which were simulated with IDA ICE. Building energy simulation involves always uncertainties, since the real behaviour of the building can differ significantly from the modelled one. Factors such as the construction process, which can affect the thermal performance of the envelope, or the real behaviour of the occupants, are always hard to predict.

Besides this common problem of building simulations, the status of the project has been a limitation. Its being still under development, meant that no final decision

on the buildings was yet made. This meant employing a model building for the simulation of the block of flats and pre-made load profiles for the office building. As much as the consumption of the block of flats is defined on the target production of the company, it is not fully representative of an actual design.

The borehole sizing has been based as well on approximations. Some data, such as the heat carrier fluid and the groundwater filling come from the common practice in the Nordics, and can be considered more reliable. Anyway, the field behaviour depends strongly on the thermal properties of the bedrock where it is installed. Here, data from nearby areas were used, but the design must be based only on specific properties of the site. Therefore, a Thermal Response Test must be carried out, so that a complete estimation of bedrock thermal properties and storing capacities is possible.

7 Conclusion

In order to face climate change, both building and energy sectors need to undergo a transition towards more sustainable solutions. Improving the energy efficiency of buildings, thus lowering their energy demand, is not sufficient alone and must go hand-in-hand with a change in energy production methods. Finland is already taking measures for the reduction of the share of fossil fuels in the energy sector and become carbon neutral by 2035. Within this background, geothermal energy and borehole thermal energy storages are becoming more and more popular. Geothermal energy can be harnessed everywhere, and its availability is not affected by the air temperature changes, which is a great advantage in a country with a climate like Finland.

This study analysed the potential of supplying a new neighbourhood primarily with geothermal energy and a low temperature distribution network. The total planned net-heated area was 111520 m^2, of which 90920 m^2 for residential use and 20600 m^2 for offices. New buildings are suitable to accommodate such systems, because floor heating requires very low temperatures to provide a comfortable indoor environment. The limitation to network supply temperature (65°C) was set by domestic hot water, which requires at least 55°C.

Simulations were conducted to analyse the system behaviour over 25 years of life span. The temperature levels in the borehole field of 154 wells suggest that the system is able to provide heating energy still after 25 years of operation. With a required output temperature set to 45°C, the heat pumps maintain efficiencies over 3 and deliver 70% of the required heat demand.

On the economical point of view, borehole thermal energy storage represents a big investment. On the other hand, savings in annual purchased energy costs are remarkable (up to 68%), as well as the reduction in the CO_2 emissions (up to 62%).

Some approximations needed to be used in the research and more detailed analysis will be required before the actual implementation of the system. However, the main aim was to provide a concept for a heating and cooling system which can supply energy in a sustainable manner.

Future research

This thesis analysed a possible configuration for a hybrid energy system. Supplemental research can be conducted on increasing the energy production on site. For example, installation of PV-panels could be used to produce a part of the electricity necessary for heat pump operation. A connection to the grid would be anyway necessary, due to the lack of solar radiation in winter when the heat demand is higher.

Further studies could concern the implementation of additional energy sources for the

backup heating, in order to reduce the dependency on district heating. For example, electric boilers are a typical backup used when operating geothermal heat pumps. One can also consider the implementation of air-to-water heat pumps as additional source of heating. Once again, the Finnish climate must be taken into account, since air-to-water heat pumps would no longer work when temperatures fall beyond -10°C. However, a combination of the three mentioned systems could be possible, together with the implementation of a proper control strategy.

Waste heat could be a potential source of energy. The office building will include laboratory units, which cooling system could reject sufficient heat to be used in soil heat regeneration or, alternatively, reused at least within the same building's heating system, e.g. for DHW pre-heating.

References

[1] IEA (2019). *Global Status Report for Buildings and Construction 2019*. URL: https://www.iea.org/reports/global-status-report-for-buildings-and-construction-2019. (accessed: Mar 20).

[2] Directorate-General for Climate Action (European Commission). *Going climate-neutral by 2050. A strategic long-term vision for a prosperous, modern, competitive and climate-neutral EU economy*. eng. Tech. rep. EU publications, 2019. DOI: 10.2834/02074.

[3] Energiateollisuus ry. *Energiavuosi 2019 - Kaukolämpö*. URL: https://energia.fi/julkaisut/materiaalipankki/energiavuosi_2019_-_kaukolampo.html#material-view. (accessed: Feb 2020).

[4] Henrik Lund et al. "4th Generation District Heating (4GDH): Integrating smart thermal grids into future sustainable energy systems". In: *Energy* 68 (2014), pp. 1–11. ISSN: 0360-5442. DOI: https://doi.org/10.1016/j.energy.2014.02.089. URL: http://www.sciencedirect.com/science/article/pii/S0360544214002369.

[5] Dietrich Schmidt and Anna Kallert. *Future Low Temperature District Heating Design Guidebook*. eng. Tech. rep. AGFW-Project Company, Frankfurt am Main, Germany, 2019. URL: https://www.iea-dhc.org/the-research/annexes/2012-2017-annex-ts1/.

[6] Dietrich Schmidt et al. "Development of an Innovative Low Temperature Heat Supply Concept for a New Housing Area". In: *Energy Procedia* 116 (2017). 15th International Symposium on District Heating and Cooling, DHC15-2016, 4-7 September 2016, Seoul, South Korea, pp. 39–47. ISSN: 1876-6102. DOI: https://doi.org/10.1016/j.egypro.2017.05.053. URL: http://www.sciencedirect.com/science/article/pii/S1876610217322609.

[7] FINVAC. *kayttoprofiilit_20140207*. URL: https://www.finvac.org/. (accessed: Oct 2019).

[8] Kaiser Ahmed, Petri Pylsy, and Jarek Kurnitski. "Hourly consumption profiles of domestic hot water for different occupant groups in dwellings". In: *Solar Energy* 137 (2016), pp. 516–530. ISSN: 0038-092X. DOI: https://doi.org/10.1016/j.solener.2016.08.033. URL: http://www.sciencedirect.com/science/article/pii/S0038092X16303711.

[9] Ari Laitinen et al. *Renewable energy production of Finnish heat pumps: Report of the SPF-project*. English. VTT Technology 164. Project code: 86237. Finland: VTT Technical Research Centre of Finland, 2014.

[10] Toivo Lapinlampi Janne Juvonen. *Energiakaivo - Maalämmön hyödyntäminen pientalossa*. Ympäristöopas 2013. Helsinki: Edita Prima Oy, 2013. ISBN: ISBN 978-952-11-4211-6.

[11] Stefan Wiemer et al. *"Good Practice" Guide for Managing Induced Seismicity in Deep Geothermal Energy Projects in Switzerland*. Tech. rep. Nov. 2017.

[12] A.-M Perttu and Signhild Gehlin. “Influence of natural convection in water-filled boreholes for GCHP”. In: *ASHRAE Transactions* 114 (Jan. 2008), pp. 416–423.

[13] Saqib Javed. “Design of ground source heat pump systems - Thermal modelling and evaluation of boreholes”. PhD thesis. Jan. 2010. DOI: 10.13140/RG.2.1.4502.8963.

[14] Per Eskilson. “Thermal analysis of heat extraction boreholes”. English. PhD thesis. Department of Physics, 1987. ISBN: 91-7900-298-6.

[15] Göran Hellström. “Ground heat storage : thermal analyses of duct storage systems”. English. PhD thesis. Mathematical Physics, 1991. ISBN: 91-628-0290-9.

[16] Y. Gu and D.L. O‘Neal. “Modeling the effect of backfills on U-tube ground coil performance”. In: (Dec. 1998). ISSN: 0001-2505.

[17] N.D. Paul. *The Effect of Grout Thermal Conductivity on Vertical Geothermal Heat Exchanger Design and Performance*. Mechanical Engineering Department, South Dakota State University, 1996. URL: https://books.google.fi/books?id=Xx6pNwAACAAJ.

[18] Mostafa H. Sharqawy, Esmail M. Mokheimer, and Hassan M. Badr. “Effective pipe-to-borehole thermal resistance for vertical ground heat exchangers”. In: *Geothermics* 38.2 (2009), pp. 271–277. ISSN: 0375-6505. DOI: https://doi.org/10.1016/j.geothermics.2009.02.001. URL: http://www.sciencedirect.com/science/article/pii/S0375650509000194.

[19] Johan Bennet, Johan Claesson, and Göran Hellström. *Multipole method to compute the conductive heat flows to and between pipes in a composite cylinder*. eng. Tech. rep. 3 - 1987. [Publisher information missing], 1987. URL: https://lup.lub.lu.se/search/ws/files/6226429/1894641.pdf.

[20] Xiaobing Liu and Göran Hellstrom. “Enhancements of an integrated simulation tool for groundsource heat pump system design and energy analysis”. In: (2006). Proceedings of Ecostock 2006, the 10th International Conference on Thermal Energy Storage, pp. 331–338.

[21] Johan Claesson and Göran Hellström. “Multipole method to calculate borehole thermal resistances in a borehole heat exchanger”. In: *HVAC&R Research* 17.6 (2011), pp. 895–911. DOI: 10.1080/10789669.2011.609927. eprint: https://www.tandfonline.com/doi/pdf/10.1080/10789669.2011.609927. URL: https://www.tandfonline.com/doi/abs/10.1080/10789669.2011.609927.

[22] BLOCON. *Earth Energy Designer*. Version 4.20. Apr. 11, 2019. URL: www.buildingphysics.com.

[23] Saqib Javed, Per Fahlén, and J Claesson. “VERTICAL GROUND HEAT EXCHANGERS: A REVIEW OF HEAT FLOW MODELS”. In: June 2009. DOI: 10.13140/RG.2.1.1465.5529.

[24] "Subsurface Heat Conduction and the Design of Borehole-Based Closed-Loop Systems". In: *An Introduction to Thermogeology: Ground Source Heating and Cooling*. John Wiley & Sons, Ltd, 2012. Chap. 10, pp. 279–324. ISBN: 9781118447512. DOI: 10.1002/9781118447512.ch10. eprint: https://onlinelibrary.wiley.com/doi/pdf/10.1002/9781118447512.ch10. URL: https://onlinelibrary.wiley.com/doi/abs/10.1002/9781118447512.ch10.

[25] "Pipes, Pumps and the Hydraulics of Closed-Loop Systems". In: *An Introduction to Thermogeology: Ground Source Heating and Cooling*. John Wiley & Sons, Ltd, 2012. Chap. 9, pp. 248–278. ISBN: 9781118447512. DOI: 10.1002/9781118447512.ch9. eprint: https://onlinelibrary.wiley.com/doi/pdf/10.1002/9781118447512.ch9. URL: https://onlinelibrary.wiley.com/doi/abs/10.1002/9781118447512.ch9.

[26] Geologian tutkimuskeskus. *Maaperä 1:100 000/Superficial deposits 1:100 000*. URL: http://gtkdata.gtk.fi/Maankamara/index.html#. (accessed: Aug 2019).

[27] Petri Hakala et al. *Evaluation of the Distributed Thermal Response Test (DTRT): Nupurinkartano as a case study*. English. Tutkimusraportti - Report of Investigation 211. Finland: GTK, 2014.

[28] Ville Lauttamäki ja Jarmo Kallio. *Geoenergiasta liiketoimintaa: perusteluja geoenergian hyödyntämiselle erilaisissa rakennuskohteissa*. Finnish. Tutkimusraportti - Report of Investigation 206. Finland: GTK, 2013.

[29] Nina Leppäharju et al. *Uuden Rakennuksen geoenergia*. Finnish. Finland: GTK, 2015.

[30] Tatu Laajalehto et al. "Energy efficiency improvements utilising mass flow control and a ring topology in a district heating network". In: vol. 69. July 2013.

[31] Uponor. *Uponor Eristetyt lämmitys- ja käyttövesiputkistot, suunnittelu ja asennus*. URL: https://www.uponor.fi/-/media/country-specific/finland/download-centre/local-heat-distribution/installation-manuals/10011_eristetyt_putkistot_09_2015.pdf?v=d7bdc6bb-42ac-4adc-a178-a577da0c7bb6. (accessed: Nov 2019).

[32] P. Nageler et al. "Novel validated method for GIS based automated dynamic urban building energy simulations". In: *Energy* 139 (2017), pp. 142–154. ISSN: 0360-5442. DOI: https://doi.org/10.1016/j.energy.2017.07.151. URL: http://www.sciencedirect.com/science/article/pii/S036054421731335X.

[33] Satu Paiho, Sakari Pulakka, and Antti Knuuti. "Life-cycle cost analyses of heat pump concepts for Finnish new nearly zero energy residential buildings". In: *Energy and Buildings* 150 (2017), pp. 396–402. ISSN: 0378-7788. DOI: https://doi.org/10.1016/j.enbuild.2017.06.034. URL: http://www.sciencedirect.com/science/article/pii/S0378778816318709.

[34] Suomen Maalämpötukku. *Finnish ground source heat wholesale.* URL: https://www.maalampotukku.fi/. (accessed: May 2020).

[35] Sebastian Herkel Franz Mauthner. *Classification and Benchmarking of Solar Thermal Systems in Urban Environments, Technical Report Subtask C – Part C1.* eng. Tech. rep. IEA, 2016. URL: https://task52.iea-shc.org/Data/Sites/1/publications/IEA-SHC-Task52-STC1-Classification-and-Benchmarking_v02.pdf.

[36] Tec Heat Ab Oy. *Maalämpö.* URL: https://www.techeat.fi/maalampo/. (accessed: May 2020).

[37] Uponor. *Uponor Ecoflex Thermo Single.* URL: https://www.uponor.fi/tuoteluettelo/eristetyt-ecoflexputkistot/tuotteet/uponor-ecoflex-thermo/uponor-ecoflex-thermo--single. (accessed: May 2020).

[38] Lassi Heikari. "System modeling and pre-feasibility analysis of local low temperature hybrid energy system; Alueellisen matalalämpötilaisen hybridi-energiajärjestelmän mallinnus ja kannattavuustarkastelu". en. G2 Pro gradu, diplomityö. 2019-08-19, pp. 94 + 13. URL: http://urn.fi/URN:NBN:fi:aalto-201908254888.

[39] European Commision. *COMMISSION DELEGATED REGULATION (EU) No 244/2012 of 16 January 2012 supplementing Directive 2010/31/EU of the European Parliament and of the Council on the energy performance of buildings by establishing a comparative methodology framework for calculating cost-optimal levels of minimum energy performance requirements for buildings and building elements.* URL: https://eur-lex.europa.eu/legal-content/EN/TXT/HTML/?uri=CELEX:32012R0244&from=EN#d1e527-18-1. (accessed: May 2020).

[40] Tilastokeskus. *Statistics Finland's PxWeb databases.* URL: http://pxnet2.stat.fi/PXWeb/pxweb/en/StatFin/. (accessed: May 2020).

[41] Nord Pool. *Historical Market Data.* URL: https://www.nordpoolgroup.com/historical-market-data/. (accessed: May 2020).

[42] Energiateollisuus ry. *Kaukolämmön hintatilasto.* URL: https://energia.fi/julkaisut/materiaalipankki/kaukolammon_hintatilasto.html. (accessed: May 2020).

[43] Janne Hirvonen and Kai Sirén. "A novel fully electrified solar heating system with a high renewable fraction - Optimal designs for a high latitude community". In: *Renewable Energy* 127 (2018), pp. 298–309. ISSN: 0960-1481. DOI: https://doi.org/10.1016/j.renene.2018.04.028. URL: http://www.sciencedirect.com/science/article/pii/S0960148118304361.

[44] Motiva. *CO2-päästökertoimet.* URL: https://www.motiva.fi/ratkaisut/energiankaytto_suomessa/co2-laskentaohje_energiankulutuksen_hiilidioksidipaastojen_laskentaan/co2-paastokertoimet. (accessed: May 2020).